Supporting Online Material for

Loss of DNA Replication Control Is a Potent Inducer of Gene Amplification

Brian M. Green, Kenneth J. Finn, Joachim J. Li*

*To whom correspondence should be addressed. E-mail: jli@itsa.ucsf.edu

Published 20 August 2010, *Science* **329**, 943 (2010)
DOI: 10.1126/science.1190966

This PDF file includes:

Materials and Methods
SOM Text
Figs. S1 to S5
Tables S1 to S9
References

SUPPLEMENTARY DISCUSSION

Our studies in budding yeast have shown that re-replication is very efficient at inducing the critical first step of gene amplification, the increase in gene copy number from one to two or more. In principal, re-replication in subsequent generations can expand copy number beyond the duplications and triplications we observed. However, once tandem copies of a large chromosomal segment are generated, other routes for expansion are available, such as nonallelic homologous recombination between sister chromatids. Hence, just inducing this first step of amplification may greatly stimulate higher order amplifications as well.

Structural analysis of the resulting amplicons as well as aCGH analysis of re-replication hint at a mechanism involving fork collapse, DNA breakage, and some type of recombinational repair at re-replication bubbles (Fig. 3D). In principle, DNA fragments with broken ends can also be generated during multiple rounds of re-replication when a re-replication fork from one round catches up to a fork from the preceding round (*S1*). However, given that only half the population of *ade3-2p* reporter cassettes re-replicated in our experimental strains and an even smaller fraction may re-replicate in more biological relevant settings (see below), we have focused on scenarios where at most one round of re-replication occurs on any molecule. Ultimately, elucidating the precise mechanism of RRIGA will require further molecular and genetic analysis of the event.

We note that, in principle, the combination of fork collapse, breakage, and repair implicated in RRIGA can also occur at replication bubbles during S phase replication. Nonetheless, re-replication appears to mobilize and coordinate these steps particularly well. Simply disrupting DNA replication with hydroxyurea or temperature sensitive replication mutations (*cdc6-1, cdc7-1, cdc9-1, or cdc17-1*) or inducing DNA breaks with the DNA damaging agent phleomycin did not result in the high levels of amplification generated by re-replication (fig. S3).

This striking efficiency of RRIGA may be due to both the nature of re-replication forks and the context in which they appear. The limited size of re-replication bubbles (apparent in Fig. 1A and fig. S2A (*S2*)) and the extensive DNA damage induced by re-replication (*S3-6*) raise the possibility that re-replication forks are more susceptible to irreversibly stalling, collapse, and breakage than replication forks. Although more detailed structural and functional studies of re-replication forks will be needed to determine if they do indeed lack the integrity of replication forks (*S7*), such a possibility could help explain why re-replication is particularly efficient at inducing the recombination events leading to gene amplifications. What is clear is that serious and highly recombinogenic fork problems can be much better tolerated during limited re-replication than they can during replication.

More sporadic problems with replication forks can occur during S phase replication, and if unresolved are thought to lead to low levels of genomic rearrangements (*S8-10*), possibly even gene amplification (*S11-13*). However, the redundancy of origins available for firing during replication provides opportunities to rescue stalled forks by converging forks originating from neighboring origins. Moreover, should these converging forks also run into problems, dormant origins may become activated in between the stalled forks to rescue both (*S14*). Hence, by

protecting themselves with multiple safeguards, cells have reduced their vulnerability to genomic rearrangements from S phase accidents. In contrast, the lack of such extensive fork backup in the context of limited re-replication, when only isolated origins re-initiate, may enhance the efficiency with which RRIGA occurs.

In essence, the loss of replication control may create a highly defective extraneous round of re-replication, providing a fertile setting for genomic rearrangement of duplicated chromosome segments, without compromising the essential first round of replication. In such a setting, it would not be surprising if other genetic alterations were also induced, such as extrachromosomal amplifications, loss of heterozygosity, aneuploidy, and translocations.

Our studies on RRIGA resurrect a model proposed nearly three decades ago for gene amplification. This re-replication model was inspired by observations of nested "onionskin" re-replication bubbles during activation of an integrated DNA tumor virus (*S15*) and during the developmentally regulated amplification of Drosophila chorion genes (*S16*). However, with limited ability to detect re-replication and no ability to induce it, direct support for the model could not be obtained, contributing to its abandonment (*S17-19*).

Also contributing to this abandonment was the rise of the breakage-fusion-bridge (BFB) model for gene amplification (fig. S5). The BFB model has since become the predominant model for intrachromosomal amplifications because various aspects of its structural signature (e.g. amplicons oriented in inverted repeat, telomeric deletions, and dicentric chromosomes) have been observed in amplifications in drug-resistant cells selected in culture, in some mouse cancer models, and in a number of human tumors (*S20*). Nonetheless, among the few tumor amplifications whose structures have been extensively characterized, there are notable examples of amplified oncogenes arranged in direct repeat (*S21-24*), which are incompatible with BFB. More recently, sequencing of breast cancer genomes has revealed hundreds of tandem duplications in direct repeat (*S25*), suggesting that duplications and higher order amplifications in direct repeat may be prevalent in cancers.

The ability of re-replication to induce amplification structures that cannot be explained by BFB suggests that RRIGA could provide a complementary gene amplification model for human tumors. Nonetheless, there are several challenges to determining whether and how much RRIGA contributes to such amplifications. First, amplicon orientation and location have not been established for most tumor-associated amplifications, so it is not yet possible to assess how many exhibit the structural signature for RRIGA versus that for BFB. Second, the minimal structural signature for RRIGA, segmental amplicons *in loco* in direct tandem repeat, is not specific to RRIGA. Even the more specific version of this signature that we observed in budding yeast, which includes repetitive elements at amplicon junctions, could arise from a nonallelic homologous recombination event that is not associated with re-replication. Hence, corroborating evidence of re-replication may be required to implicate RRIGA in tumors.

Detecting such re-replication will likely require the development of more sensitive replication assays. Standard assays in current use, such as flow cytometry and density shift have difficulty detecting re-replication that increases DNA content by less than 5-10%. Compounding this detection problem is the likelihood that only extremely low or sporadic levels of re-

replication will contribute to genomic instability. Currently detectable levels of re-replication cause widespread cell death or apoptosis (*S3-6, 26-28*), presumably because of the extensive DNA damage it causes (*S3-6*). In fact, the very limited re-replication occurring in our MC_{2A} strains (Fig. 1A and fig. S2A) was both undetectable by flow cytometry (although detectable by our more sensitive aCGH assay) and too lethal for sustained induction. We had to transiently induce re-replication in order to see the massive stimulation of gene amplification that is possible in these strains.

We thus suspect that the most likely pathological context for RRIGA to occur will involve mutations that constitutively disrupt replication control just enough to take advantage of the extreme efficiency of RRIGA but not enough to significantly compromise viability. In effect, currently undetectable levels of re-replication could provide an oncogenic "mutator" phenotype (*S29*). The difficulty of detecting re-replication in this context could account for why re-replication has not been widely reported in tumor cells or cell lines susceptible to gene amplification. It may also explain why modest overexpression of the replication proteins Cdt1 or Cdc6 can potentiate oncogenesis in mice without causing overt re-replication (*S30-32*). Interestingly, if more sensitive replication assays do eventually demonstrate that some tumors are associated with low levels of re-replication, one can imagine that these tumor cells might be especially vulnerable to therapeutic agents that incrementally deregulate replication control further, thereby increasing re-replication in these cells to highly lethal levels.

Finally, given that gene copy number increases are important in the diversification and evolution of species (*S33, 34*), it is tempting to revive speculation that sporadic re-replication might contribute to evolutionary changes as well (*S35*). Recent studies suggest that the fidelity of wild type DNA polymerases are less than maximal, possibly to ensure sufficient genetic plasticity for evolutionary change (*S36*). It is conceivable that replication controls in eukaryotic cells are similarly tuned below maximal stringency to facilitate adaptive genomic alterations on an evolutionary time scale.

SUPPLEMENTARY MATERIALS AND METHODS

Oligonucleotides. Oligonucleotides used in the plasmid and yeast strain constructions described below as well as the PCR analysis of amplicon boundaries and junctions are listed in Table S7.

Plasmids. All plasmids used for strain construction are listed in Table S8. The plasmids containing the *ade3-2p* copy number reporter cassette (schematized in fig. S1A) are described below.

Plasmids pBJL2890 and pBJL2892 effectively consist of the following fragments of DNA: Homology Left (SacI to StuI of PCR product from YJL4489 (*S2*) genomic DNA using OJL1796 and OJL1797 for pBJL2890 and OJL1804 and OJL1805 for pBJL2892), a StuI-PmeI linker sequence (5'-AGGCCTGTTTAAAC-3'), kanMX6 (PmeI to XmaI of pFA6a-pGAL1-3HA (*S37*)), *ade3-2p* (XmaI to SgrAI of pDK243 (*S38*)), an SgrAI-XbaI linker sequence (5'-CACCGGCGTCTAGA-3'), *ARS317* (SpeI to XbaI of PCR product from S288c genomic DNA using OJL1794 and OJL1795 cloned into pCR2.1 TA TOPO, which picks up part of the polylinker including the XbaI site 5'-GTTTAAACCCATTTGAGCAAGGGCGAATTCTGCAGATATCCATCACACTGGCGGCCGCTCGAGCATGCATCTAGA-3'), Homology Right (XbaI to NotI of PCR product from YJL4489 (*S2*) genomic DNA using OJL1798 and OJL1799 for pBJL2890 and OJL1806 and OJL1807 for pBJL2892), a NotI-SalI linker sequence (5'-GCGGCCGCGTCGAC-3') and vector backbone (SalI to SacI of pRSS56 (*S39*)).

Plasmids pBJL2889 and pBJL2891 consist of the same fragments as pBJL2890 and pBJL2892, respectively, except they lack the *ARS317* fragment. Plasmid pBJL2876 has the same cassette lacking *ARS317* but the Homology Left fragment was amplified from yeast genomic DNA using OJL1684 and OJL1685 and the Homology Right fragment was amplified using OJL1686 and OJL1687.

For all plasmids, a SacI to SalI fragment spanning the inserted sequences from Homology Left to Homology Right was used in the strain constructions described below.

Strains. All strains used in this study have their genotypes listed in Table S9. Re-replicating strains were derived from YJL3758 (*MATa MCM7-2NLS ura3-52::{pGAL-ΔntCDC6-cdk2A, URA3} ORC2 ORC6 leu2 trp1-289 ade2 ade3 bar1::LEU2*). YJL3758 was in turn derived as follows from YJL1737 (*MATa orc2-cdk6A orc6-cdk4A ura3-52 leu2 trp1-289 ade2 ade3 bar1::LEU2*) (*S40*). YJL2067 was generated from YJL1737 by loop-in/loop-out gene replacement of *MCM7* with *MCM7-2NLS* using Asp1-linearized pJL1206 (*S40*). YJL3151 was generated from YJL2067 by loop-in/loop-out gene replacement of *orc2-6A* with *ORC2-(Not1,SgrAI)* using EcoNI-linearized pMP933 (*S40*); *ORC2-(Not1,SgrAI)* is a phenotypically wild-type version of *ORC2* containing 5'-ATGGCACCGGTGGGCGGCCGC-3' inserted just upstream of the ORF ATG and is referred to simply as *ORC2* in strain genotypes. YJL3155 was generated from YJL3151 by loop-in/loop-out gene replacement of *orc6-4A* with *ORC6* using SphI-linearized pJL737 (*S40*). YJL3758 was generated from YJL3155 by loop-in integration of StuI-linearized pJL1488 (*S2*) *(pGAL1-ΔntCDC6-cdk2A*) at *ura3-52*.

(Correction added in proofs. YJL3155, YJL3758 and all re-replicating strains derived from YJL3758 were discovered to have one Orc6 CDK consensus site still mutated (codon ACG for Serine 116 mutated to codon GCG for Alanine 116). Although CDK consensus mutations N- and C-terminal to this site were converted back to wild-type during loop-in/loop-out with

pJL737, this site in the middle somehow was not. Genotypes in Table S9 have been corrected where appropriate by including the allele orc6-cdk1A$_{116}$. When we reconstructed a true MC2A strains with fully wild-type ORC6, we found that it still preferentially re-initiates ARS317 but the level of re-initiation is 3-fold lower than the MC2A orc6-cdk1A$_{116}$ background used in the experiments published here.)

YJL6558 and YJL6561, re-replicating strains with an *ade3-2p* reporter cassette containing *ARS317*, were generated from YJL3758 by the integration of the SacI to SalI fragment from pBJL2890 or pBJL2892, respectively, into Chromosome IV followed by disruption of the endogenous *ARS317* with a PCR product of natMX derived from pAG25 (*S41*) using OJL1639 and OJL1640. Chromosome IV, the largest chromosome in *Saccharomyces cerevisiae*, was chosen as the integration site for the reporter cassettes because *ade3-2p* duplication is least likely to arise from re-replication of the entire chromosome initiated at the cassette. The endogenous *ARS317* on chromosome III was deleted to minimize additional gross chromosomal alterations that could be stimulated by re-replication at this site.

YJL6555 and YJL6557, re-replicating strains with an *ade3-2p* reporter cassette lacking *ARS317*, were generated from YJL3758 by the integration of the SacI to SalI fragment from pBJL2889 or pBJL2891, respectively, followed by disruption of the endogenous *ARS317* with the PCR product of natMX described above.

The non-rereplicating strains, YJL6974 and YJL6977, were derived from YJL3756 (*MATa MCM7-2NLS ORC2 orc6-cdk1A116 ura3-52::{pGAL, URA3} leu2 trp1-289 ade2 ade3 bar1::LEU2*), by the integration of the SacI to SalI fragment from pBJL2890 or pBJL2892, respectively, followed by disruption of the endogenous *ARS317* with the PCR product of natMX described above. YJL3756 was generated from YJL3155 by loop-in integration of StuI-linearized pJL806 (*S40*) (*pGAL1*) at the *ura3-52* locus.

YJL6032, a strain used as a source of reference DNA for some of the aCGH analysis, was derived from YJL3758 by integration of the SacI to SalI fragment from pBJL2876. This introduces a *ade3-2p* reporter cassette without *ARS317* about 5 kb centromere distal to the endogenous *ARS317*. YJL7695, another strain used as a source of reference DNA for some of the aCGH analysis, was derived from YJL6974 by loop-out removal of pJL806, followed by loop-in/loop-out replacement of MCM7-2NLS with MCM7 using BamHI-linearized pJL1033 (*S42*).

YJL7007, a wild-type diploid used to analyze the effect of hydroxyurea and phleomycin on gene amplification, was generated as follows. The mating type of YJL3155 (*MATa MCM7-2NLS ORC2 orc6-cdk1A$_{116}$ ura3-52 leu2 trp1-289 ade2 ade3 bar1::LEU2*) was switched using *pGAL-HO* in pSB283 (*S43*) to form YJL3165. In both YJL3155 and YJL3165, *MCM7-2NLS* was converted back to *MCM7* by loop-in/loop-out gene replacement using BamHI-linearized pJL1033 to generate YJL3516 and YJL3519, respectively. An *ade3-2p ARS317* reporter cassette was introduced into YJL3516 by integration of the SacI to SalI fragment from pBJL2890 to generate YJL6993. YJL3519 and YJL6993 were mated to generate YJL7007.

Strains used to study the effects of *cdc* mutants on gene amplification were generated as follows. For the wild-type *CDC* control, an *ade3-2p ARS317* reporter cassette (SacI to SalI fragment of pBJL2980) was integrated into 4541-8-1 (*S44*) (*MATα leu2 ade2 ade3 his7 sap3 gal1 ura1 can1*). In parallel, a *MATa* version of 4541-8-1 was generated by mating type switching using *pGAL-HO* in pSB283 (*S43*). Mating of the two strains generated YJL7002. YJL7003, YJL7005, YJL7006, and YJL7087 were similarly generated using different starting strains described in Palmer et al. (*S44*): YJL7003 was derived from 4525-061 (*MATα cdc6-1*

leu2 ade2 ade3 his7 sap3 gal1 can1); YJL7005 was derived from 4528-091 (*MATα cdc9-1 leu2 ade2 ade3 his7 sap3 gal1 ura1 can1*); YJL7006 was derived from 4532-171 (*MATα cdc17-1 leu2 ade2 ade3 his7 sap3 gal1 ura1 can1*); and YJL7087 was derived from 4524-1-3 (*MATα cdc7-1 leu2 ade2 ade3 his7 sap3 gal1 ura1 can1*).

YJL7443 and YJL7452 were generated from YJL6558 by the integration of a *TRP1* disruption fragment to replace *DNL4* or *RAD52*, respectively. *TRP1* disruption fragments were generated using PCR in two steps. Step 1 primers (see table S7) were used to amplify *TRP1* from pRS304 (*S39*) and add short regions of homology flanking either *DNL4* or *RAD52*. Step 2 primers extended the region of homology, using the PCR product obtained in Step 1 as a template.

Strain Growth and Induction of Re-Replication, DNA Damage, or Replication Stress. Cells were grown in or on YEP or synthetic complete (SC) medium supplemented with 2% wt/vol dextrose (to form YEPD or SDC) or 3% wt/vol raffinose + 0.05% wt/vol dextrose (to form YEPRaf or SRafC). For synthetic medium, 1x amino acid concentrations were as described by Sherman (*S45*) except the amount of leucine was doubled to 60 μg/ml and the amount of serine was halved to 200 μg/ml. With the exception of plates for red/pink colony color development, all synthetic medium contained 2x amino acids. Color development plates contained 1x amino acids except 0.5x adenine (10 μg/ml). All cell growth was performed at 30°C except where otherwise noted.

To obtain reproducible induction of re-replication, cells were diluted from a fresh unsaturated culture grown in YEPD into YEPRaf and allowed to grow exponentially for 12–15 h overnight till they reached an OD_{600} of 0.2 -0.8. At this cell density, 15ug/ml nocodazole (Sigma M1404 or US Biological N3000) was added for 120-150 min to arrest cells in G2/M phase. The *GAL1* promoter (*pGAL1*) was then induced by addition of 2-3% galactose for 3 hr. Tight maintenance of the arrest was confirmed by quantifying the percent of large budded cells (buds with diameters > 0.5x mother cell diameter) and analyzing the distribution of total DNA content by flow cytometry as previously described (*S46*).

To perturb S phase replication, the indicated *cdc* mutant strains were grown exponentially overnight in YEPD at 23°C to an OD_{600} 0.2 – 0.8, then shifted to 36°C or 30°C for 3 or 6 hr, respectively. Alternatively, a wild type *CDC* strain was grown exponentially overnight in YEPD at 30°C to an OD_{600} 0.2 – 0.8, then 0.2M or 0.1M hydroxyurea (US Biological H9120) was added for 3 or 6 hr, respectively. To induce DNA damage, cells were grown exponentially in YEPD at 30°C overnight to an OD_{600} 0.2 – 0.8, then 2 μg/ml or 20 μg/ml phleomycin (Invivogen ant-ph-1) was added for 3 hr. The effect of these treatments on cell cycle progression was monitored by quantifying the percent of large budded cells and analyzing the distribution of total DNA content by flow cytometry as previously described (*S46*)

Colony Sectoring Assay. To score the frequency of red sectors, ~200 colonies were plated per SDC plates containing limiting (0.5x) adenine. Temperature sensitive strains were grown for 7-10 days at 23°C and other strains were grown at 30°C for 5 days. Then cells were shifted to 23°C for 2-6 days till colony color development was optimal. Plates were randomized and scored blind. Red sectors were counted if: 1) the sectors were greater than 1/8 of the colony, 2) darker red than the neighboring colonies (i.e., not a pink sector in a nearly white colony) and 3) the junctions between the red sector and pink colony were largely straight, to minimize sectors due to poor growth. The frequency of sectored colonies was determined by dividing the total

sector counts by the total number of viable colonies. This frequency was measured in at least two independent induction experiments, and the mean and standard error of the mean are reported (see table S1).

We cannot be sure whether red sectors between 1/8 and 1/2 of the colony arose because persistence of ΔntCdc6-cdk2A allowed residual re-replication to occur after release from the nocodazole arrest or because re-replication bubbles generated during the nocodazole arrest can somehow be propagated for a few generations before being converted to a stable gene amplification. Nonetheless, it is clear that re-replication induced an increase in the number of all red sectors 1/8 and larger (Fig. 1B), and that most of these displayed segmental amplifications.

Amplification Frequency and Rate. The amplification frequencies arising from re-replication of the *ade3-2p* cassette at $ChrIV_{567kb}$ for YJL6974, YJL6555, and YJL6558 were calculated by multiplying their sector frequencies (table S1) by the fraction of red sectors containing *ade3-2p* amplifications, as determined by CGH. These fractions were 3/32, 1/6, and 31/35, yielding amplification frequencies of 1.3×10^{-4}, 9.7×10^{-4}, and 3.0×10^{-2}, for YJL6974, YJL6555, and YJL6558, respectively.

Frequencies of genomic instability reported in the literature have often been converted to rates by using Lea and Coulson's method of the median (*S47*), an approximation of Luria-Delbruck fluctuation analysis. Fluctuation analysis, however, applies to constitutive rates of mutations, which generate fluctuations in the frequency of accumulated mutations because mutations that appear earlier during population growth contribute more mutants to the population than mutations acquired later. Fluctuation analysis does not apply and is not needed for mutations induced by transient genetic perturbations. In the simplest case of a perturbation that is experienced within a single generation and causes mutations in just that generation, the rate of mutation (per generation) would equal the observed frequency of mutation. For our RRIGA analysis, re-replication was induced within a single cell cycle, and amplifications acquired over the three immediately following generations were scored, so the observed amplifications could be attributed to a specific pulse of re-replication. Thus, we divided the observed frequency of 3.0×10^{-2} for YJL6558 by three generations to obtain an order of magnitude RIGGA rate of 10^{-2} per generation.

Pulsed Field Gel Electrophoresis. Cells were prepared for pulsed field gel electrophoresis as described (*S4*). Plugs were cut in half and loaded on a 1% SeaKem LE agarose (wt/vol) gel in 1x TAE (40 mM Tris, 40 mM acetate, and 2 mM EDTA, pH 8.0). Electrophoresis was carried out at 14°C in 1x TAE on a CHEF DR-III system with a switch time of 500 s, run time of 48 hr, voltage of 3 V, and angle of 106°. The DNA was transferred as described (*S4*) and probed with an *ADE3* probe generated by PCR of pBJL2889 with oligonucleotides OJL1757 and OJL1758.

Genomic DNA Preparation for aCGH Analysis

Method 1: ~10 OD_{600} units of yeast were collected for DNA preparation. With the exception of samples for YJL7452 sector isolates, cultures were grown in YEPD and were either arrested with α-factor (40-50 ng/ml) or nocodazole (10-15 μg/ml), or were grown to saturation in YEP + 7-8% dextrose. YJL7452 isolates arrested poorly under all conditions, so samples were collected from asynchronous populations. In all cases DNA was prepared using the MasterPure Yeast DNA Purification Kit (Epicentre, Madison, WI), according to the manufacturer's instructions.

aCGH performed with this DNA generates data points with greater scatter than DNA prepared by Method 2, but is still reliable for mapping quantal copy number changes.
Method 2: 250 ml of culture (arrested with either α-factor or nocodazole as described above) was mixed with 1.2 ml of 20% sodium azide and added to 25 ml of frozen, -80°C, 0.2 M EDTA, 0.1% sodium azide. Cells were pelleted, washed with 50 ml 4°C TE (10 mM Tris-Cl, 1 mM EDTA pH 7.5) and stored frozen at -80°C. Pellets were resuspended in 4 ml Lysis buffer (2% Triton X-100, 1% SDS, 100 mM NaCl, 10 mM Tris-Cl, 1 mM EDTA pH 8.0) and mixed with 4 ml of phenol:$CHCl_3$:isoamyl alcohol (25:24:1) and 8 ml 0.5 mm glass beads (BioSpec Products, Inc., Bartlesville, OK). The suspension was vortexed seven times for 2-3 min separated by 2-3 min intervals at RT to get at least 95% of the cells lysed. The lysate was diluted with 8 ml phenol:$CHCl_3$:isoamyl alcohol (25:24:1) and 8 ml TE, vortexed once more**,** and then centrifuged at 18,500 x g for 15 min at RT. After collecting the aqueous phase, the interphase was re-extracted with 8 ml TE, and the second aqueous phase from this re-extraction pooled with the first. The combined aqueous phases were extracted with an equal volume of $CHCl_3$. The bulk of the RNA in the extract was selectively precipitated by addition of 0.01 volume 5 M NaCl (to a final concentration of 50 mM) and 0.4 volumes isopropanol followed by centrifugation at 9,000 x g for 15 min at RT. The RNA pellet was discarded and an additional 0.4 volumes of isopropanol was added to the supernatant to precipitate the DNA. Following centrifugation at 9,000 x g for 15 min at RT, the pellet was washed with 70% ethanol, dried, and resuspended with 3.5 ml of 10 mM Tris-Cl (pH 8), 1 mM EDTA. RNase A (Qiagen, Valencia, CA) was added to 340 μg/ml and the sample incubated at 37ºC for 30 min. Then Proteinase K was added to 555 μg/ml followed by another incubation at 55°C for 30 min. Finally, 0.5 ml of 10% (w/v) Cetyltrimethylammonium Bromide (CTAB, Sigma H6269), 0.9 M NaCl (prewarmed to 65°C) and 0.9 ml of 5 M NaCl was added. The sample was incubated for 20 min at 65°C before being extracted with 8 ml $CHCl_3$:isoamyl alcohol (24:1) and centrifuged at 6000 x g for 15 min at RT. The DNA in the aqueous phase was precipitated with 0.8 volumes isopropanol at RT, washed with 70% ethanol, dried, and resuspended in 6 ml of 25 mM Tris-Cl (pH 7), 1 mM EDTA. RNase A (Qiagen, Valencia, CA) was added to 33 μg/ml and the sample incubated at 37ºC for 15 min. Then the following were added to the sample in the order listed: 1) 1.5 ml of 5 M NaCl; 2) 0.5 ml of 1M MOPS (pH 7); 3) 0.5 ml of Triton X-100 (3% vol/vol); 4) 1.5 ml of isopropanol. The sample was then mixed by vortexing, then purified on a Qiagen Genomic-tip 100/G column as per the manufacturer's instructions (Qiagen, Valencia, CA). The eluted DNA was precipitated with 0.8 volumes isopropanol at 4°C, washed with 70% ethanol, dried, and resuspended in 275 µl of 2 mM Tris-Cl pH 7.8. Genomic DNA was then sheared by sonication with a Branson Sonifier 450 to an average fragment size of 500 bp. This method of DNA preparation was used for all aCGH profiles shown in the figures.

aCGH Analysis of Gene Amplification. For DNA purified by Method 1, 80-100% of each DNA sample was labeled with Cy3 and 1.5-2ug of purified reference DNA from YJL6032 or YJL6558 was labeled with Cy5 essentially as described (*S2*). The labeled DNA was isolated using one of two previously described methods (low-throughput (*S2*) or high-throughput (*S48*)). For DNA prepared by Method 2, 2-2.5μg of each DNA sample was labeled with Cy5 and 1.5-2μg of purified reference DNA from YJL6032, YJL6974, or YJL7695 was labeled with Cy3 essentially as described (*S2*), and labeled DNA was isolated as previously described (*S2*). All samples were hybridized and analyzed as described (*S2*). All microarray data is deposited with

the Gene Expression Omnibus (http://www.ncbi.nlm.nih.gov/geo/) with accession number GSE22018.

aCGH Analysis of Re-replication. Re-replication profiles were performed by aCGH as described above, using Method 2 for DNA preparation. Because aCGH reports on a population average of DNA copy number, re-replication of a locus in a small percentage of cells (we estimate < 5-10%) would probably not register as a significant copy number increase above the 2C baseline of M phase arrested cells. Hence, although *ARS317* is the predominant origin re-initiating in MC2A strains, the lethality that persists when *ARS317* is absent from the genome (data not shown), suggests that other origins throughout the genome may be firing below the sensitivity of detection for aCGH. All microarray data is deposited with the Gene Expression Omnibus (http://www.ncbi.nlm.nih.gov/geo/) with accession number GSE22018.

Junction PCR. PCR amplification of the amplicon junctions required special care because of the large repetitive Ty element(s) at each junction. DNA was prepared from 5 ml of saturated culture using a modified Winston-Hoffman DNA prep (*S49*). Cells were pelleted in a screw cap tube and resuspended in 200 μl of Winston-Hoffman Lysis buffer (2% Triton X-100, 1% SDS, 100mM NaCl, 10mM Tris.Cl pH8.0, 1mM EDTA pH8.0). 200 μl of glass beads and 200 μl of phenol:$CHCl_3$:isoamyl alcohol (25:24:1) were added and the tubes were vortexed in a Tomy multi mixer (setting of 7) for 10 min at room temperature. 450 µl 1x TE was added to each tube, which were then mixed well and microfuged at 20,000 x g for 3 min. 500 μl of the aqueous layer was transferred to new screw cap tube containing 10 μl of RNase A (10 mg/ml) and incubated at 23°C for 2 hours. 300 μl of phenol:$CHCl_3$:isoamyl alcohol (25:24:1) was added to each tube, which were then vortexed in the Tomy mixer for 5 min and microfuged at 20,000 x g for 3 min. 400 μl of the aqueous layer was transferred to new Eppendorf tubes containing 300 μl chloroform, vortexed, and microfuged at 20,000 x g for 3 min. 300 μl of the aqueous layer was transferred to new Eppendorf tubes containing 3 μl 10N ammonium acetate pH 7.0 and 750 μl 100% ethanol. Tubes were vortexed, then microfuged at 20,000 x g for 7 min. The DNA pellet was washed with 300 μl of 70% ethanol, dried and resuspended in 50 μl of 1x TE. 0.5 μl of DNA was subjected to PCR with 2.5 μl Roche Long Template Buffer, 1.25 μl 10 μM of each oligo, 2.5 μl 5mM dNTPs, 1.25 U Roche Expand polymerase and H_2O to a final volume of 25 μl. The PCR conditions were 94°C for 3 min, then 30 cycles of 94°C for 30 sec, 60°C for 1 min, 68°C for 15 min, and finally 68°C for 10 min.

The oligonucleotide primers used for these PCR reactions are listed in Table S7. As schematized in Figure 2B, these primers hybridize to unique sequences close to either side of the Ty elements that array CGH data suggested would be at or near the boundaries of the amplicons. Primers 1_{515} and 2_{515} flank YDRCTy2-1 at Chr IV 515kb, which mapped close to the left boundary of all amplicons. Primers 3_{650} and 4_{650} flank YDRCTy1-1 at Chr IV 650kb, which mapped close to the right boundary of all but one amplicon analyzed by PCR (YJL7110). Primers 3_{985} and 4_{985} flank the inverted Ty pair of YDRWTy2-3 and YDRCTy1-3 at Chr IV 985kb, which mapped close to the rightmost boundary of the amplicon in YJL7110.

For all strains analyzed by PCR except YJL7110, if the amplicons were in direct repeat due to nonallelic homologous recombination between YDRCTy2-1 and YDRCTy1-1, the prediction is that they would successfully yield PCR products for primer sets 1_{515} and 2_{515} (8016 bp), 3_{650} and 4_{650} (6494 bp), and 2_{515} and 3_{650} (7564 bp) and no PCR product for primers 2_{515} alone or 3_{650} alone. In all cases except one the presence and size of the products from these five PCR

reactions matched this prediction, and a representative set of these products from one strain is shown in Fig. 2B. For the one exception, YJL7095, no product was obtained for the interamplicon junction PCR involving primers 2_{515} and 3_{650}. We note that the aCGH data indicate that the amplification is complex, with some regions triplicated and others duplicated, and thus cannot be unequivocally defined using this PCR approach.

For YJL7110, the structural premise that best fits the data is a direct repeat of amplicons formed by nonallelic homologous recombination between YDRWdelta7 at Chr IV 520kb and YDRWdelta20 near Chr IV 985kb (which is part of the inverted Ty elements YDRWTy2-3 and YDRCTy1-3 at Chr IV 985kb). Such a premise predicts PCR products for primer sets 1_{515} and 2_{515} (8016 bp), 3_{985} and 4_{985} (12110 bp), and 2_{515} and 3_{985} (6339 bp) and no PCR product for primers 2_{515} alone or 3_{985} alone. The presence and size of the PCR products matched these predictions, and sequencing of the interamplicon junction PCR product (as described below) from primers 2_{515} and 3_{985} confirmed a crossover between the two delta elements as proposed (data not shown).

Inter-amplicon Junction Sequencing. Genomic DNA was prepared from YJL7101, YJL7102, YJL7103, and YJL7104 (see table S9) using a modified Winston-Hoffman DNA prep (*S49*), as described above for Junction PCR using oligonucleotide primers 2_{515} and 3_{650}. PCR reactions were cleaned up using a Qiagen PCR Clean-up kit, according to the manufacturer's instructions (Qiagen, Valencia, CA). Cleaned up PCR products were sequenced by MCLabs (South San Francisco, CA) using oligonucleotides described in Table S7. Sequence analysis was performed using Vector NTI software (Invitrogen, Carlsbad, CA).

SUPPLEMENTARY FIGURE LEGENDS

Figure S1. Screening for re-replication induced gene amplification using colony sectoring.

A) Integrated copy number reporter cassette consists of the kanMX marker, *ade3-2p* copy number reporter gene, and several hundred base pairs of homology to the left (dark grey box) and right (light grey box) of the desired integration site (see Supplementary Methods). Two versions of the cassette were used: (top) one containing an *ARS317* fragment that preferentially re-initiates in the *MC2A* re-replicating strain background, and (bottom) one lacking the *ARS*.

B) Schematic of gene amplification screen. Cells were induced to re-replicate for 3 hr at a G2/M phase arrest then plated for single colonies on plates that remove the induction for re-replication and allow colony color development. Parental cells with a single copy of the *ade3-2p* cassette are pink. Cells in a colony lineage that acquire a stable heritable amplification of the *ade3-2p* reporter gene will generate a red sector, whose size reflects when the amplification occurred. Shown is an example of a colony where the *ade3-2p* cassette was stably amplified by one cell at the four-cell stage, resulting in a pink colony with a red quarter sector. Pink colonies with 1/2, 1/4, and 1/8 red sectors were streaked to colony purify red cells. Red sectors that successfully restreaked were quantified and their genomic DNA analyzed by aCGH to determine if they indeed had amplified their reporter cassette. Sectoring was a good indicator of cassette amplification in cells that re-initiated *ARS317* on the *ade3-2p* cassette (Fig. 1C, fig. S2B, table S2 and S3). However, color development is affected by other factors besides *ade3-2p* copy number. In other settings, such as in non-rereplicating strains (table S4), strains perturbed by DNA damage (fig. S3C and table S5), or re-replicating strains with a *RAD52* deletion (Fig. 3C and table S6), red sectors usually did not contain amplification of the *ade3-2p* cassette and presumably arose from other genetic alterations.

Figure S2. Re-replication from $ChrIV_{1089kb}$ induces primary gene amplification

A) Induction of re-replication at $ChrIV_{1089kb}$. Strains containing an *ade3-2p* copy number reporter cassette integrated at $ChrIV_{1089kb}$ were arrested in G2/M phase and treated with galactose for 3 hr to trigger re-initiation of *ARS317*. Copy number analysis of re-replication (>2C) by aCGH is shown for Chr IV. All other chromosomes maintained a copy number at or close to 2C (data not shown). Top panel: YJL6977, non-re-replicating strain with *ARS317* in *ade3-2p* cassette (*MATa MCM7-2NLS orc6-cdk1A$_{116}$ ura3-52::{pGAL, URA3} ChrIV$_{1089kb}$::{ade3-2p, ARS317, kanMX} ade2 ade3 ars317Δ::natMX*). Middle panel: YJL6557, re-replicating strain with no *ARS317* in *ade3-2p* cassette (*MATa MCM7-2NLS orc6-cdk1A$_{116}$ ura3-52::{pGAL-ΔntCDC6-cdk2A, URA3} ChrIV$_{1089kb}$::{ade3-2p, kanMX} ade2 ade3 ars317Δ::natMX*). Bottom panel: YJL6561, re-replicating strain with *ARS317* in *ade3-2p* cassette (*MATa MCM7-2NLS orc6-cdk1A$_{116}$ reura3-52::{pGAL-ΔntCDC6-cdk2A, URA3} ChrIV$_{1089kb}$::{ade3-2p, ARS317, kanMX} ade2 ade3 ars317Δ::natMX*).

B) Re-replication of the *ade3-2p* reporter cassette stimulates colony sectoring at $ChrIV_{1089kb}$.

YJL6977, YJL6557, and YJL6977 were treated as described in A. After 0 or 3 hr galactose induction, isolated cells were plated for single colonies on media containing dextrose to block further re-replication and limiting adenine to promote color development (see fig. S1B). The frequency of pink colonies with 1/2, 1/4, or 1/8 red sectors were then quantified (mean ± SEM, N = 2 to 3 induction replicates; see table S1).

C) Red sectors induced by re-replication at $ChrIV_{1089kb}$ display primary gene amplifications. 24 red sectors derived from YJL6561 were analyzed by aCGH and distributed into seven classes based on the copy number profile of Chr IV (see table S3). Chr IV profiles of the two largest classes are shown. Schematic of Chr IV shows positions of Ty elements (triangles), centromere (circle), and *ade3-2p* cassette (black bar). * boundary maps to Ty LTR element and not full Ty element in genome sequence of *S. cerevisiae*, S288c (*S50*). † boundary does not map to any full Ty or LTR element present in the genome sequence of *S. cerevisiae*, S288c (*S50*); whether the boundary coincides with an unmapped Ty or LTR element in YJL6561, which has a different strain background derived from A364a and W303, was not determined.

Figure S3. Specificity of primary gene amplifications induced by re-replication.

A) Replication mutants did not generate frequent red sectors. Diploid strains YJL7002 (*WT*), YJL7003 (*cdc6-1/cdc6-1*), YJL7087 (*cdc7-1/cdc7-1*), YJL7005 (*cdc9-1/cdc9-1*), and YJL7006 (*cdc17-1/cdc17-1*), all containing $ChrIV_{567kb}$*::{ade3-2p, ARS317, kanMX}* on one homolog were grown exponentially at 23° C then shifted to restrictive temperatures (36° C) for 3 hr or semipermissive temperatures (30° C) for 6 hr to perturb DNA replication. Cells were plated and red sectors quantified (mean ± SEM, N = 2 induction replicates; see table S1) as described in Fig. 1B with results for YJL6558 shown for comparison. % large budded cells were quantified right before plating to monitor the effectiveness of the *cdc* perturbation.

B) HU induced replication stress did not generate frequent red sectors. Exponentially growing WT diploid YJL7007 were treated with 0.1 M or 0.2 M HU for the indicated times then plated and red sectors quantified (mean ± SEM, N = 2 to 3 induction replicates; see table S1) as described in Fig. 1B with results for YJL6558 shown for comparison. % large budded cells were quantified right before plating to monitor the effectiveness of the HU treatment.

C) DNA damage induced chromosomal fragmentation. Exponentially growing WT diploid cells (YJL7007, *MATa/MATα MCM7/MCM7 ORC2/ORC2 ORC6/ORC6 ChrIV/*$ChrIV_{567kb}$*::{ade3-2p, ARS317, kanMX}*) were treated with indicated concentrations of phleomycin for 3 hr before chromosomes were analyzed by PFGE and ethidium bromide staining.

D) DNA damage induced red sectoring. YJL7007 (WT) cells treated as described in C were plated for red sectored colonies and quantified (mean ± SEM, N = 2 to 3 induction replicates; see table S1) as described in Fig. 1B with results for YJL6558 shown for comparison. % large budded cells were quantified right before plating to confirm induction of the DNA damage response.

E) Red sectors induced by DNA damage did not display gene amplification. Representative aCGH profile of Chr IV displayed by 24/24 red sectors obtained from treatment of YJL7007 with 20 μg/ml phleomycin as described in D (see table S5).

Figure S4. Sequence of hybrid Ty elements at interamplicon junctions.

YJL7101-7104 contain amplicons bounded by YDRCTy2-1 at $ChrIV_{515kb}$ and YDRCTy1-1 at $ChrIV_{650kb}$. Hybrid Ty elements at the interamplicon junctions were amplified by PCR and sequenced. Shown is the left most (centromere proximal) segment of approximately 1.4 kb, which spans the region where YDRCTy2-1 and YDRCTy1-1 share 99% identity (unboxed sequence). Crossover events were detected as transitions from sequence specific to YDRCTy1-1 (grey box) to sequence specific to YDRCTy2-1 (white box). Additional sequence obtained to the left and right of the displayed sequence are consistent with crossovers in these isolates only occurring in this region (data not shown). To the left of all four isolates, we sequenced at least 170 bp that proved to be identical to genomic sequences centromere proximal to the endogenous YDRCTy1-1. Similarly, in all four isolates we sequenced at least 560 bp to the right that turned out to be identical to YDRCTy2-1. For two of the isolates, YJL7103 and YJL7104, the rightward sequence continued all the way past the end of the hybrid Ty element and this sequence was shown to be identical to YDRCTy2-1 and the centromere distal genomic sequence flanking this Ty element at its endogenous location. * marks the position of every tenth nucleotide.

Figure S5. Breakage-fusion-bridge model

A schematic of a breakage fusion bridge cycle is shown. Breakage through both sister chromatids, or a break in G1 phase of the cell cycle followed by chromatid replication, (upper left) can result in fusion of the two sisters in inverted orientation (upper right). Such a fusion, which can also be initiated by telomere erosion, results in a dicentric chromosome. Attempts to segregate the two centromeres generate a mitotic bridge (lower right) and often results in breakage between the centromeres. The larger chromosome fragment contains an inverted duplication of part of the region centromeric to the original break and is missing the region telomeric to that break (lower left). Replication of this DNA results in two sister chromatids each with a break, allowing the cycle to be repeated multiple times (upper left) until a telomere is finally captured by one of the broken ends.

Figure S1

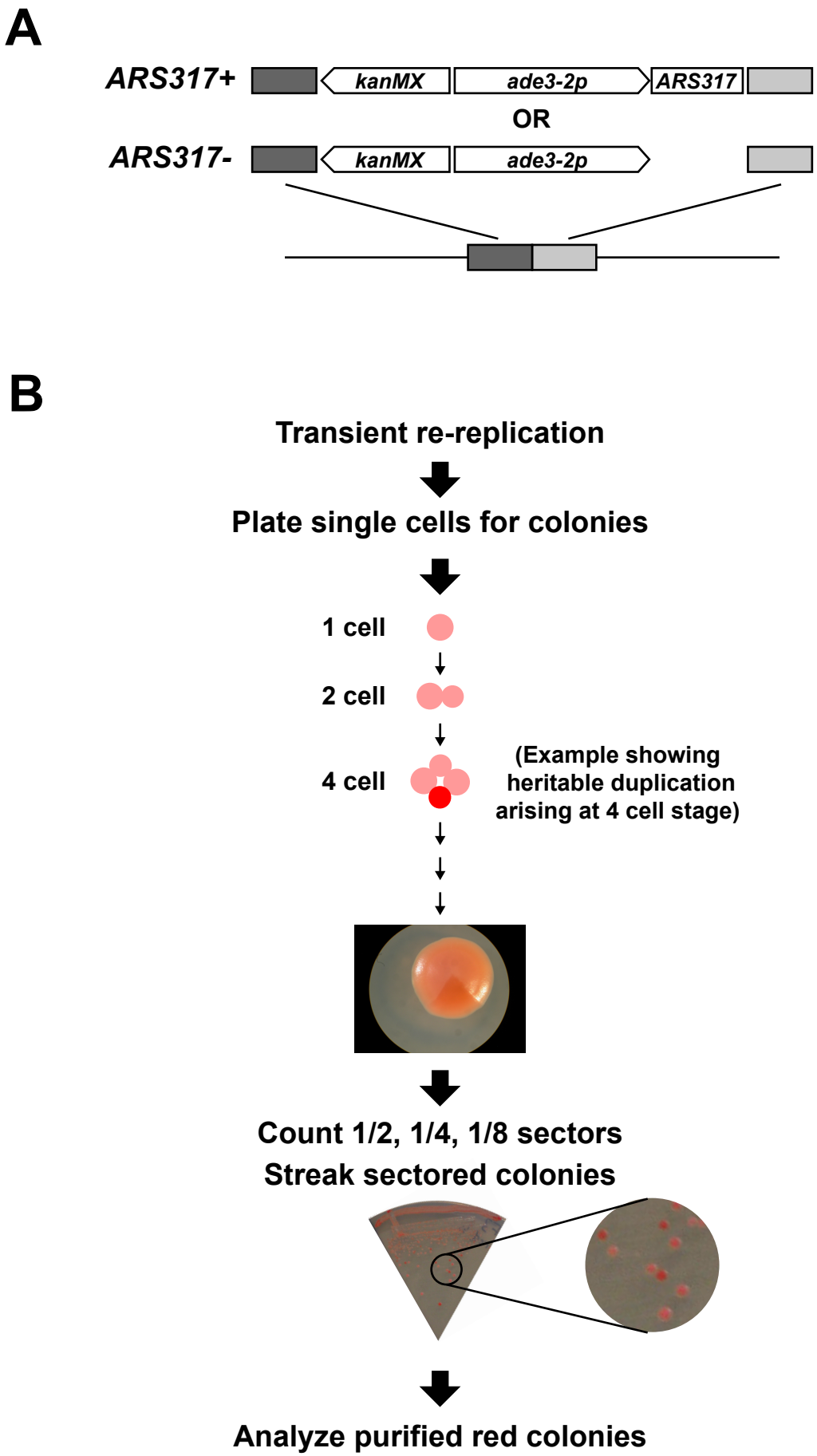
A
ARS317+
kanMX
ade3-2p
ARS317
OR
ARS317-
kanMX
ade3-2p
B
Transient re-replication
Plate single cells for colonies
1 cell
2 cell
4 cell
(Example showing heritable duplication arising at 4 cell stage)
Count 1/2, 1/4, 1/8 sectors
Streak sectored colonies
Analyze purified red colonies

Figure S2

A

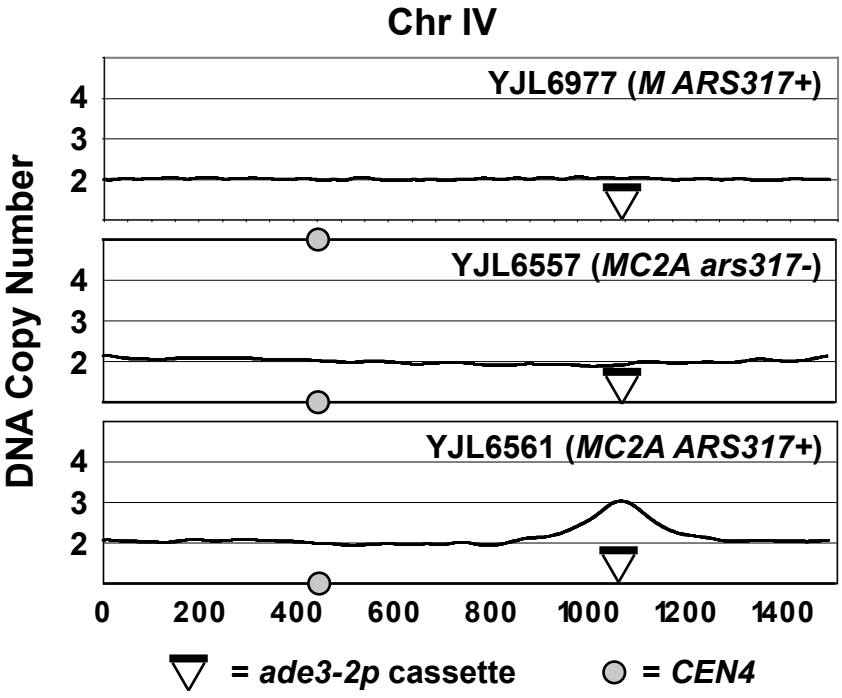

B

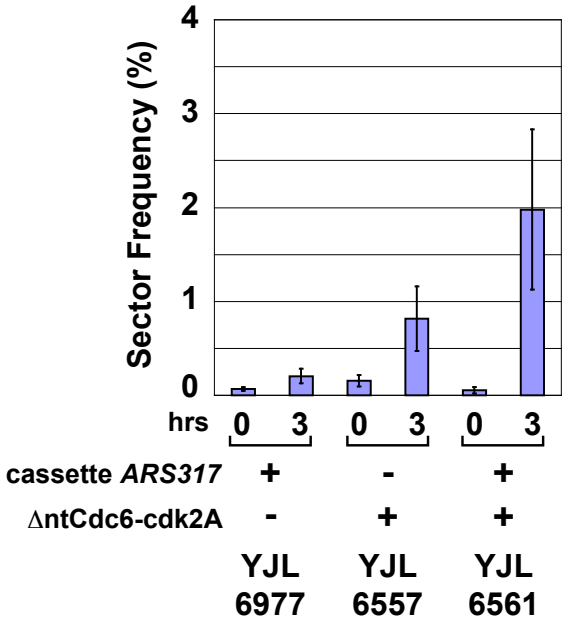

C

CGH Analysis of YJL6561 Sectors

# Isolates	# Amplicons	Boundaries (kb)
9	2	985 to 1205
3	2	985 to 1350*
1	2	985 to 1150*
1	2	875 to 1205
1	2	805* to 1205
1	2	925† to 1350*
8	1	n/a

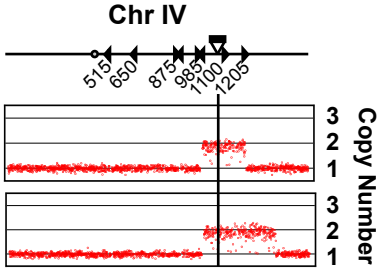

Figure S3

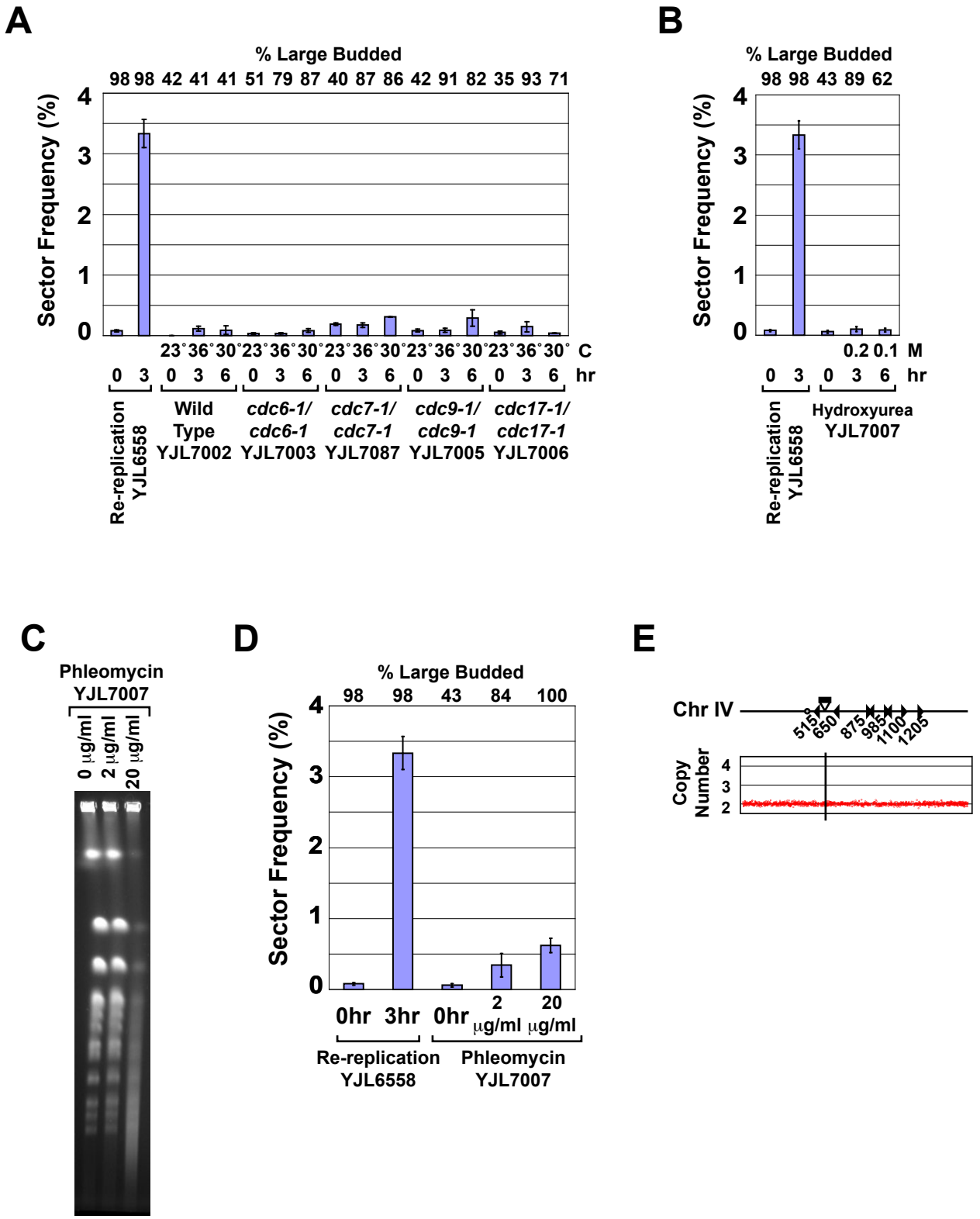
A
% Large Budded
98 98 42 41 41 51 79 87 40 87 86 42 91 82 35 93 71
Sector Frequency (%)
23° 36° 30° 23° 36° 30° 23° 36° 30° 23° 36° 30° 23° 36° 30° C
0 3 0 3 6 0 3 6 0 3 6 0 3 6 0 3 6 hr
Re-replication YJL6558
Wild Type YJL7002
cdc6-1/ cdc6-1 YJL7003
cdc7-1/ cdc7-1 YJL7087
cdc9-1/ cdc9-1 YJL7005
cdc17-1/ cdc17-1 YJL7006
B
% Large Budded
98 98 43 89 62
Sector Frequency (%)
0.2 0.1 M
0 3 0 3 6 hr
Re-replication YJL6558
Hydroxyurea YJL7007
C
Phleomycin YJL7007
0 μg/ml
2 μg/ml
20 μg/ml
D
% Large Budded
98 98 43 84 100
Sector Frequency (%)
0hr 3hr 0hr 2 μg/ml 20 μg/ml
Re-replication YJL6558
Phleomycin YJL7007
E
Chr IV
515 650 875 985 1100 1205
Copy Number

Figure S4

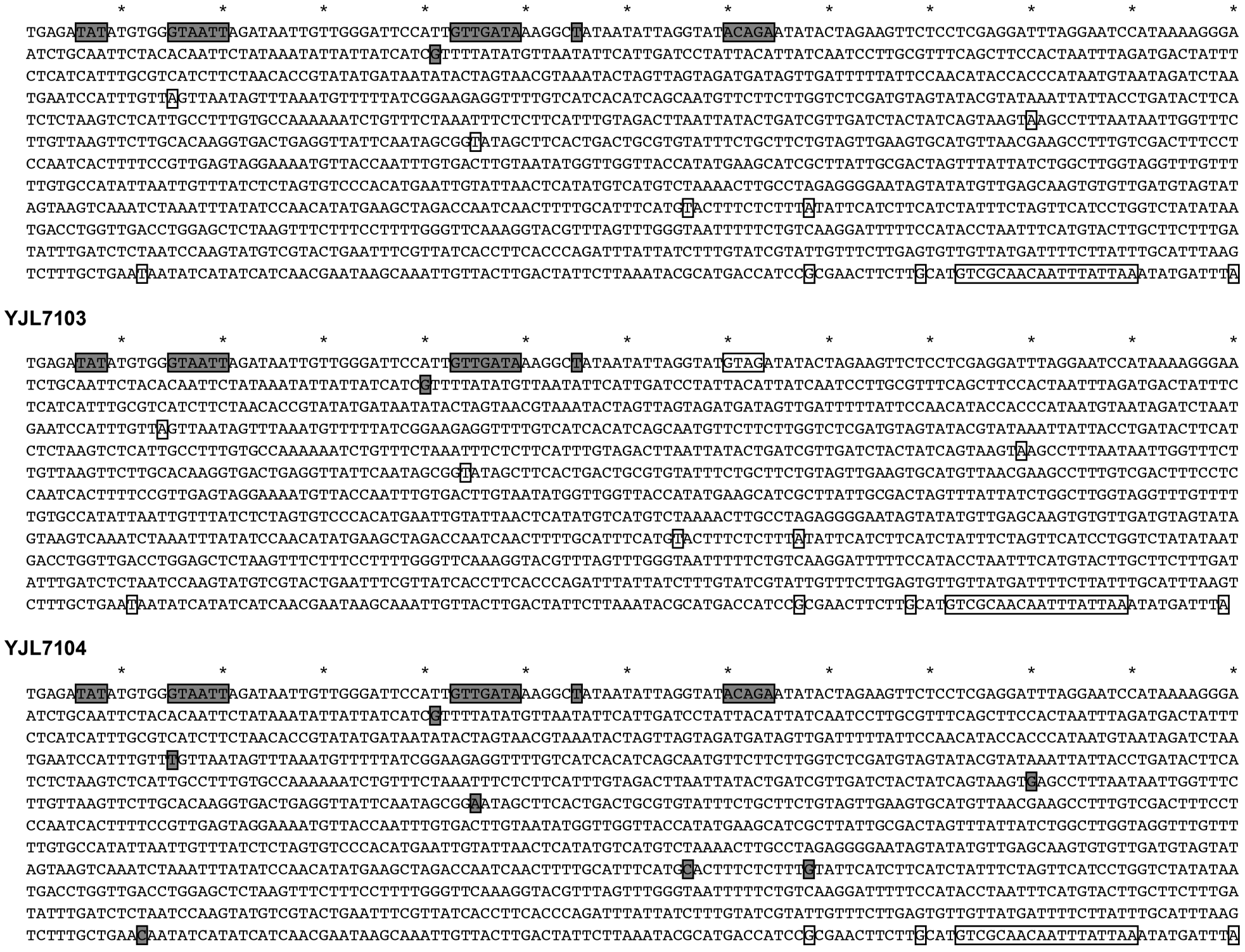

Figure S5

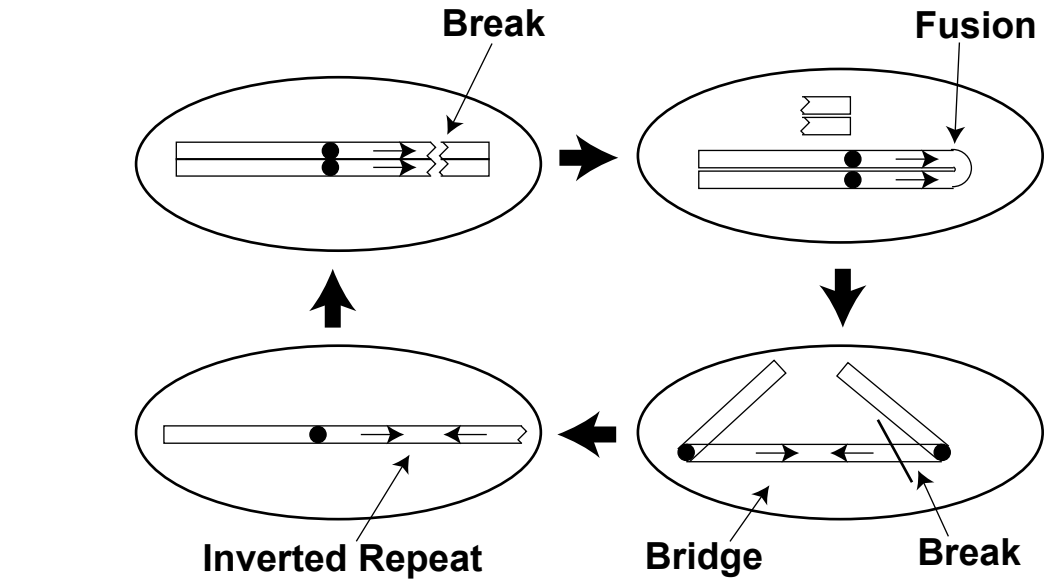
Break
Fusion
Inverted Repeat
Bridge
Break
Loss of Chromosome Distal to Repeat

Table S1

Frequency of 1/2, 1/4, and 1/8 red sectored colonies observed in this work

Parent Strain	Genotype	Cassette	Conditions	# Trials	Total Colonies Screened	Mean Sector Frequency	Standard Error of the Mean
YJL6974	*MCM7-2NLS pGAL*	*ChrIV:567kb ade3-2p ARS317*	Nocodazole Arrest + 0 hr Galactose	4	15243	0.04%	0.008%
YJL6974	*MCM7-2NLS pGAL*	*ChrIV:567kb ade3-2p ARS317*	Nocodazole Arrest + 3 hr Galactose	4	30453	0.14%	0.030%
YJL6555	*MCM7-2NLS pGAL-ΔntCDC6-cdk2A*	*ChrIV:567kb ade3-2p*	Nocodazole Arrest + 0 hr Galactose	2	8612	0.05%	0.005%
YJL6555	*MCM7-2NLS pGAL-ΔntCDC6-cdk2A*	*ChrIV:567kb ade3-2p*	Nocodazole Arrest + 3 hr Galactose	2	17076	0.58%	0.258%
YJL6558	*MCM7-2NLS pGAL-ΔntCDC6-cdk2A*	*ChrIV:567kb ade3-2p ARS317*	Nocodazole Arrest + 0 hr Galactose	7	22922	0.08%	0.017%
YJL6558	*MCM7-2NLS pGAL-ΔntCDC6-cdk2A*	*ChrIV:567kb ade3-2p ARS317*	Nocodazole Arrest + 3 hr Galactose	7	21754	3.34%	0.232%
YJL6977	*MCM7-2NLS pGAL*	*ChrIV:1089kb ade3-2p ARS317*	Nocodazole Arrest + 0 hr Galactose	2	14176	0.07%	0.021%
YJL6977	*MCM7-2NLS pGAL*	*ChrIV:1089kb ade3-2p ARS317*	Nocodazole Arrest + 3 hr Galactose	2	13488	0.20%	0.075%
YJL6557	*MCM7-2NLS pGAL-ΔntCDC6-cdk2A*	*ChrIV:1089kb ade3-2p*	Nocodazole Arrest + 0 hr Galactose	3	14728	0.15%	0.059%
YJL6557	*MCM7-2NLS pGAL-ΔntCDC6-cdk2A*	*ChrIV:1089kb ade3-2p*	Nocodazole Arrest + 3 hr Galactose	3	20762	0.82%	0.345%
YJL6561	*MCM7-2NLS pGAL-ΔntCDC6-cdk2A*	*ChrIV:1089kb ade3-2p ARS317*	Nocodazole Arrest + 0 hr Galactose	3	11544	0.05%	0.034%
YJL6561	*MCM7-2NLS pGAL-ΔntCDC6-cdk2A*	*ChrIV:1089kb ade3-2p ARS317*	Nocodazole Arrest + 3 hr Galactose	3	13450	1.98%	0.855%
YJL7007	*WT/WT*	*ChrIV:567kb ade3-2p ARS317*	Asynchronous*	3	15788	0.06%	0.022%
YJL7007	*WT/WT*	*ChrIV:567kb ade3-2p ARS317*	Asyncrhonous + 3 h 2 µg/ml Phleomycin	2	10454	0.34%	0.167%
YJL7007	*WT/WT*	*ChrIV:567kb ade3-2p ARS317*	Asyncrhonous + 3 h 20 µg/ml Phleomycin	2	9088	0.62%	0.100%

Table S1 (continued)

Frequency of 1/2, 1/4, and 1/8 red sectored colonies observed in this work

Parent Strain	Genotype	Cassette	Conditions	# Trials	Total Colonies Screened	Mean Sector Frequency	Standard Error of the Mean
YJL7002	*WT/WT*	*ChrIV:567kb ade3-2p ARS317*	Asynchronous (22° C)	2	4451	0.00%	0.000%
YJL7002	*WT/WT*	*ChrIV:567kb ade3-2p ARS317*	Asynchronous (22° C) + 3 h 36° C	2	5419	0.11%	0.040%
YJL7002	*WT/WT*	*ChrIV:567kb ade3-2p ARS317*	Asynchronous (22° C) + 6 h 30° C	2	8240	0.09%	0.071%
YJL7003	*cdc6-1/cdc6-1*	*ChrIV:567kb ade3-2p ARS317*	Asynchronous (22° C)	2	10416	0.03%	0.014%
YJL7003	*cdc6-1/cdc6-1*	*ChrIV:567kb ade3-2p ARS317*	Asynchronous (22° C) + 3 h 36° C	2	8208	0.04%	0.010%
YJL7003	*cdc6-1/cdc6-1*	*ChrIV:567kb ade3-2p ARS317*	Asynchronous (22° C) + 6 h 30° C	2	11168	0.08%	0.030%
YJL7087	*cdc7-1/cdc7-1*	*ChrIV:567kb ade3-2p ARS317*	Asynchronous (22° C)	2	5840	0.19%	0.022%
YJL7087	*cdc7-1/cdc7-1*	*ChrIV:567kb ade3-2p ARS317*	Asynchronous (22° C) + 3 h 36° C	2	7952	0.17%	0.039%
YJL7087	*cdc7-1/cdc7-1*	*ChrIV:567kb ade3-2p ARS317*	Asynchronous (22° C) + 6 h 30° C	2	7144	0.31%	0.004%
YJL7005	*cdc9-1/cdc9-1*	*ChrIV:567kb ade3-2p ARS317*	Asynchronous (22° C)	2	5136	0.08%	0.022%
YJL7005	*cdc9-1/cdc9-1*	*ChrIV:567kb ade3-2p ARS317*	Asynchronous (22° C) + 3 h 36° C	2	10224	0.09%	0.036%
YJL7005	*cdc9-1/cdc9-1*	*ChrIV:567kb ade3-2p ARS317*	Asynchronous (22° C) + 6 h 30° C	2	8448	0.29%	0.134%
YJL7006	*cdc17-1/cdc17-1*	*ChrIV:567kb ade3-2p ARS317*	Asynchronous (22° C)	2	7520	0.05%	0.024%
YJL7006	*cdc17-1/cdc17-1*	*ChrIV:567kb ade3-2p ARS317*	Asynchronous (22° C) + 3 h 36° C	2	6576	0.15%	0.084%
YJL7006	*cdc17-1/cdc17-1*	*ChrIV:567kb ade3-2p ARS317*	Asynchronous (22° C) + 6 h 30° C	2	4816	0.04%	0.001%

Table S1 (continued)

Frequency of 1/2, 1/4, and 1/8 red sectored colonies observed in this work

Parent Strain	Genotype	Cassette	Conditions	# Trials	Total Colonies Screened	Mean Sector Frequency	Standard Error of the Mean
YJL7007	*WT/WT*	*ChrIV:567kb ade3-2p ARS317*	Asynchronous*	3	15788	0.06%	0.022%
YJL7007	*WT/WT*	*ChrIV:567kb ade3-2p ARS317*	Asyncrhonous + 3 h 0.2M Hydroxyurea	2	7384	0.10%	0.040%
YJL7007	*WT/WT*	*ChrIV:567kb ade3-2p ARS317*	Asyncrhonous + 6 h 0.05M Hydroxyurea	2	7952	0.08%	0.028%
YJL7443	*dnl4Δ MCM7-2NLS pGAL-ΔntCDC6-cdk2A*	*ChrIV:567kb ade3-2p ARS317*	Nocodazole Arrest + 0 hr Galactose	2	6593	0.08%	0.030%
YJL7443	*dnl4Δ MCM7-2NLS pGAL-ΔntCDC6-cdk2A*	*ChrIV:567kb ade3-2p ARS317*	Nocodazole Arrest + 3 hr Galactose	2	8569	2.91%	0.020%
YJL7452	*rad52Δ MCM7-2NLS pGAL-ΔntCDC6-cdk2A*	*ChrIV:567kb ade3-2p ARS317*	Nocodazole Arrest + 0 hr Galactose	2	7244	0.18%	0.020%
YJL7452	*rad52Δ MCM7-2NLS pGAL-ΔntCDC6-cdk2A*	*ChrIV:567kb ade3-2p ARS317*	Nocodazole Arrest + 3 hr Galactose	2	31883	0.25%	0.040%

* Same set of experiments used as asynchronous untreated control for both Phleomycin and Hydroxyurea experiments

Table S2

Analysis of sectored colonies generated by re-replicating strain containing reporter cassette at Chr IV_{567kb} (YJL6558).

Sectored Colony	Copy Number (CGH)	Amplicon Boundaries (CGH)	Chr IV Size Status (PFGE)	Chr IV Expected kb Increase	Direct Repeat (Jxn PCR)	Other CGH Changes
YJL7095	3 2	515 to 650 650 to 670	Increased	290	-	None
YJL7096	2	515 to 650	Increased	135	+	None
YJL7097	2	515 to 650	Increased	135	+	None
YJL7098	2	515 to 650	Increased	135	+	None
YJL7099	2	515 to 650	Increased	135	+	None
YJL7100	1	n/a	No change	0	ND	Chr V disomy
YJL7101	2	515 to 650	Increased	135	+	None
YJL7102	2	515 to 650	Increased	135	+	None
YJL7103	2	515 to 650	Increased	135	+	None
YJL7104	2	515 to 650	Increased	135	+	None
YJL7105	2	515 to 650	Increased	135	+	None
YJL7106	1	n/a	No change	0	ND	None
YJL7107	2	515 to 650	Increased	135	+	None
YJL7108	2	515 to 650	Increased	135	+	None
YJL7109	2	515 to 650	Increased	135	+	None
YJL7110	2	515 to 985	Increased	470	+	None
YJL7111	2	515 to 650	Increased	135	+	None
YJL7112	2 2	515 to 650 875 to 985	Increased	245	+	None
YJL7113	1	n/a	No change	0	ND	None
YJL7114	2	515 to 650	Increased	135	+	None
YJL7115	2	515 to 650	Increased	135	+	None
YJL7116	2	515 to 650	Increased	135	+	None
YJL7117	2	515 to 650	Increased	135	+	Chr III disomy
YJL7118	1	n/a	No change	0	ND	None
YJL7556	2	515 to 650	ND	ND	ND	None
YJL7557	2	515 to 650	ND	ND	ND	None
YJL7558	2	515 to 650	ND	ND	ND	None
YJL7559	2	515 to 650	ND	ND	ND	None
YJL7584	2	515 to 875	ND	ND	ND	None
YJL7585	2	515 to 650	ND	ND	ND	None
YJL7586	2	515 to 650	ND	ND	ND	None
YJL7587	2	515 to 650	ND	ND	ND	None
YJL7689	2	515 to 650	ND	ND	ND	None
YJL7690	2	515 to 650	ND	ND	ND	None
YJL7691	3	515 to 650	ND	ND	ND	None

Copy Number and Amplicon Boundaries refer to locus encompassing reporter cassette. Boundaries are reported as kilobases (kb) from the left telomere of ChrIV. Boudaries correspond to the position of Ty elements (515=Ty2; 650=Ty1; 875=Ty1; 985=Ty1) or LTRs (670=δ) mapped for S288c on the Saccharomyces Genome Database. Boundary numbers were used to calculate the expected size increase in ChrIV after all amplifications screened by PFGE were shown to be intrachromosomal. Direct Repeat refers to whether junction PCR (see Fig. 2) confirmed the presence of a head-to-tail amplicon junction. The one negative (YJL7095) may have failed because we used PCR primers to detect a junction between 515 kb and 650 kb and not a junction between 515 kb and 670 kb. n/a- not applicable; ND - not done.

Table S3

CGH analysis of sectored colonies generated by re-replicating strain containing reporter cassette at Chr IV_{1089kb} (YJL6561).

Sectored Colony	Copy Number	Amplicon Boundaries	Other CGH Changes
YJL7119	2	805 to 1205	None
YJL7120	2	985 to 1205	None
YJL7121	2	875 to 1205	None
YJL7122	2	985 to 1205	None
YJL7123	2	985 to 1205	None
YJL7124	1	n/a	Chr X segmental duplication, 200kb to 355kb
YJL7125	1	n/a	Chr V disomy
YJL7126	2	985 to 1350	None
YJL7127	2	985 to 1205	None
YJL7128	2	985 to 1205	Chr V partial disomy, left TEL to 285kb Chr XVI partial disomy, left TEL to 100kb
YJL7129	2	985 to 1205	None
YJL7130	1	n/a	Chr II disomy
YJL7131	2	985 to 1205	None
YJL7132	1	n/a	None
YJL7133	2	985 to 1205	None
YJL7134	1	n/a	Chr V disomy
YJL7135	2	985 to 1350	None
YJL7136	2	985 to 1350	None
YJL7137	2	925 to 1350	None
YJL7138	1	n/a	None
YJL7139	2	985 to 1205	None
YJL7140	1	n/a	None
YJL7141	1	n/a	Chr II disomy
YJL7142	2	985 to 1150	None

Copy Number and Amplicon Boundaries refer to locus encompassing the reporter cassette. n/a - not applicable. Boundaries are reported as kilobases (kb) from the left telomere of ChrIV and correspond to the position of Ty elements (875=Ty2; 985=Ty2; 1205=Ty1) or LTRs (805=δ; 1150=δ; 1350=δ) mapped for S288c on the Saccharomyces Genome Database, except for 925kb. TEL is yeast telomere sequences.

Table S4

CGH analysis of sectored colony isolates generated by non-re-replicating strain containing reporter cassette at $ChrIV_{567kb}$ (YJL6974).

Sectored Colony	Copy Number	Amplicon Boundaries	Other CGH Changes
YJL7548	1	n/a	Chr V disomy
YJL7549	1	n/a	Chr II partial disomy, left TEL to 260kb Chr III partial disomy, 170 kb to right TEL
YJL7550	1	n/a	Chr V disomy
YJL7551	2	515 to 875	None
YJL7552	1	n/a	Chr V disomy
YJL7553	1	n/a	Chr XIII disomy
YJL7554	1	n/a	None
YJL7555	1	n/a	Chr V disomy
YJL7560	1	n/a	Chr II disomy
YJL7561	1	n/a	Chr II disomy
YJL7562	1	n/a	Chr XIII disomy
YJL7563	1	n/a	Chr XIII disomy
YJL7564	1	n/a	Chr II disomy Chr III disomy
YJL7565	1	n/a	Diploid Chr I monosomy Chr III trisomy
YJL7566	1	n/a	Chr II disomy Chr XVI disomy
YJL7567	1	n/a	Chr II disomy
YJL7568	1	n/a	Chr III disomy
YJL7569	1	n/a	Chr V disomy
YJL7570	1	n/a	Chr IV disomy
YJL7571	1	n/a	Chr V disomy
YJL7572	2	515 to 985	None
YJL7573	1	n/a	Chr V disomy Chr XIII disomy Chr XVI disomy
YJL7574	1	n/a	Chr V disomy
YJL7575	1	n/a	Chr XIII disomy
YJL7576	1	n/a	None
YJL7577	1	n/a	Chr II disomy
YJL7578	1	n/a	Chr II disomy
YJL7579	1	n/a	None
YJL7580	1	n/a	Chr II disomy
YJL7581	1	n/a	Chr II disomy
YJL7582	2	515 to 650	None
YJL7583	1	n/a	Chr II disomy Chr V disomy

Copy Number and Amplicon Boundaries refer to locus encompassing the reporter cassette. Boundaries are reported as kilobases (kb) from the left telomere of ChrIV and correspond to the position of Ty elements (515=Ty2; 650=Ty1; 875=Ty1; 985=Ty1) identified for S288c in the Saccharomyces Genome Database. n/a - not applicable. TEL - telomere.

Table S5

CGH analysis of sectored colonies generated by DNA damage from 20 µg/ml phleomycin in diploid strain containing reporter cassette at 567kb on one homolog of ChrIV (YJL7007).

Sectored Colony	Diploid Copy Number	Amplicon Boundaries	Other CGH Changes
YJL7143	2	n/a	Chr VI partial monosomy, left arm Chr III partial trisomy, left arm
YJL7144	2	n/a	None
YJL7145	2	n/a	None
YJL7146	2	n/a	Chr V partial monosomy, right arm Chr V partial trisomy, left arm
YJL7147	2	n/a	Chr V trisomy
YJL7148	2	n/a	None
YJL7149	2	n/a	None
YJL7150	2	n/a	None
YJL7151	2	n/a	None
YJL7152	2	n/a	Chr VIII monosomy
YJL7153	2	n/a	Chr V partial monosomy, right arm Chr XIII partial trisomy, right arm
YJL7154	2	n/a	Chr IV partial trisomy, right arm Chr XVI partial monosomy, left arm
YJL7155	2	n/a	None
YJL7156	2	n/a	Chr V partial trisomy, left arm Chr V segmental duplication Chr VII segmental deletion Chr XV partial monosomy, right arm
YJL7157	2	n/a	None
YJL7158	2	n/a	None
YJL7159	2	n/a	Chr I monosomy
YJL7160	2	n/a	None
YJL7161	2	n/a	None
YJL7162	2	n/a	Chr I monosomy
YJL7163	2	n/a	Chr III partial trisomy, left arm Chr III partial monosomy, right arm
YJL7164	2	n/a	None
YJL7165	2	n/a	None
YJL7166	2	n/a	Chr I partial trisomy, right arm Chr III partial monosomy, left arm Chr VIII monosomy

Diploid Copy Number and Amplicon Boundaries refer to locus encompassing the reporter cassette. Unamplified diploid copy number is 2. No boundaries are reported because no amplification of the reporter cassette was observed. n/a is not applicable.

Table S6

CGH analysis of sectored colonies generated in *rad52*Δ (YJL7452) and *dnl4*Δ (YJL7443) re-replicating strains containing reporter cassette at ChrIV$_{567kb}$.

Colony Isolate	Parent Strain	Copy Number	Amplicon Boundaries	Other CGH Changes
YJL7609	YJL7452	1	n/a	None
YJL7610	YJL7452	1	n/a	None
YJL7611	YJL7452	1	n/a	Chr II disomy
YJL7612	YJL7452	1	n/a	None
YJL7613	YJL7452	1	n/a	None
YJL7614	YJL7452	1	n/a	None
YJL7615	YJL7452	1	n/a	None
YJL7616	YJL7452	1	n/a	None
YJL7617	YJL7452	1	n/a	None
YJL7618	YJL7452	1	n/a	Chr XIII disomy
YJL7619	YJL7452	1	n/a	None
YJL7620	YJL7452	1	n/a	None
YJL7621	YJL7452	1	n/a	None
YJL7622	YJL7452	1	n/a	None
YJL7623	YJL7452	1	n/a	None
YJL7624	YJL7452	1	n/a	None
YJL7625	YJL7452	1	n/a	None
YJL7626	YJL7452	1	n/a	None
YJL7627	YJL7452	1	n/a	Chr XIII disomy
YJL7628	YJL7452	1	n/a	None
YJL7629	YJL7452	1	n/a	None
YJL7630	YJL7452	1	n/a	None
YJL7631	YJL7452	1	n/a	Chr XIII disomy
YJL7632	YJL7452	1	n/a	None
YJL7633	YJL7452	1	n/a	None
YJL7634	YJL7452	1	n/a	None
YJL7635	YJL7452	1	n/a	None
YJL7636	YJL7452	1	n/a	None
YJL7637	YJL7452	1	n/a	None
YJL7638	YJL7452	1	n/a	None
YJL7639	YJL7452	1	n/a	None
YJL7640	YJL7452	1	n/a	None
YJL7641	YJL7452	1	n/a	None
YJL7642	YJL7452	2	515 to 590	None
YJL7643	YJL7452	1	n/a	None
YJL7644	YJL7452	1	n/a	Diploid Chr I monosomy
YJL7645	YJL7452	1	n/a	None
YJL7646	YJL7452	1	n/a	None
YJL7647	YJL7452	1	n/a	None
YJL7648	YJL7452	1	n/a	None
YJL7649	YJL7452	1	n/a	None
YJL7650	YJL7452	1	n/a	None

Table S6 (continued)

CGH analysis of sectored colonies generated in *rad52*Δ (YJL7452) and *dnl4*Δ (YJL7443) re-replicating strains containing reporter cassette at $ChrIV_{567kb}$.

Colony Isolate	Parent Strain	Copy Number	Amplicon Boundaries	Other CGH Changes
YJL7651	YJL7452	2	515 to 580	None
YJL7652	YJL7452	1	n/a	None
YJL7653	YJL7452	1	n/a	None
YJL7654	YJL7452	1	n/a	None
YJL7655	YJL7452	1	n/a	None
YJL7656	YJL7452	1	n/a	None
YJL7657	YJL7443	2	515 to 650	None
YJL7658	YJL7443	2	515 to 650	None
YJL7659	YJL7443	2	515 to 650	None
YJL7660	YJL7443	2	515 to 650	None
YJL7661	YJL7443	2	515 to 650	None
YJL7662	YJL7443	1	n/a	Chr V segmental duplication, 60kb to 110kb
YJL7663	YJL7443	2	515 to 650	None
YJL7664	YJL7443	2	515 to 650	None
YJL7665	YJL7443	2	515 to 650	None
YJL7666	YJL7443	2	515 to 650	None
YJL7667	YJL7443	2	515 to 985	None
YJL7668	YJL7443	2	515 to 650	None
YJL7669	YJL7443	2	515 to 650	None
YJL7670	YJL7443	2	515 to 650	None
YJL7671	YJL7443	2	515 to 650	None
YJL7672	YJL7443	2	515 to 650	None
YJL7673	YJL7443	2	515 to 650	None
YJL7674	YJL7443	2	515 to 650	None
YJL7675	YJL7443	2	515 to 650	None
YJL7677	YJL7443	2	515 to 875	Chr V segmental duplication, 290kb to 445kb
YJL7685	YJL7443	2	515 to 875	None
YJL7686	YJL7443	1	n/a	None
YJL7687	YJL7443	2	515 to 650	None
YJL7688	YJL7443	2	515 to 650	None

Copy Number and Amplicon Boundaries refer to locus encompassing the reporter cassette. Boundaries are reported as kilobases (kb) from the left telomere of ChrIV. Boudaries correspond to the position of Ty elements (515=Ty2; 650=Ty1; 875=Ty1; 985=Ty1) mapped for S288c on the Saccharomyces Genome Database, except for 580kb and 590kb. n/a - not applicable

Table S7

Oligonucleotides used in this study. Listed 5' to 3', left to right. Uppercase letters indicate sequence that anneals to the template during PCR or sequencing.
Lowercase letters indicate sequence added by PCR, either to provide homology for genomic integration or to provide restriction sites for cloning.
Subscript numbers are nucleotide coordinates provided by the Saccharomyces Genome Database (Nov 2009)

Name	Sequence	Purpose
OJL1639	attaaacaatgtttgatttttaaatcgcaatttaataccCGGATCCCCGGGTTAATTAA	*ars317::NatMX*
OJL1640	atttttatggaagattaagctcataacttggacggggatcCATCGATGAATTCGAGCTCG	*ars317::NatMX*
OJL1684	gatcgagctcccgcggGGTAGTCTTGCAAAGGTGTG	*ChrIII*$_{296334-296955}$ *for pBJL2876*
OJL1685	gatcgtttaaacaggcctCAAGAGTGCATGTAATGTTT	*ChrIII*$_{296334-296955}$ *for pBJL2876*
OJL1686	gatccaccggcgtctagaGGAGTAAGCTGCATCATAAT	*ChrIII*$_{296956-297810}$ *for pBJL2876*
OJL1687	gatcgtcgacgcggccgcTATTGGAAAAGGTTACTTGG	*ChrIII*$_{296956-297810}$ *for pBJL2876*
OJL1757	CAAAAGCATTCAAGGTCACG	*ADE3* probe
OJL1758	TCAATTCGCCAATGTTGGTG	*ADE3* probe
OJL1794	gctcaaatgggtttaaacACTAGTACTTAAAAAAACTG	*ARS317* for cloning
OJL1795	gctcaaatgggtttaaacCCAGGAGTACCTGCGCTTAT	*ARS317* for cloning
OJL1796	gctcaaatggaagcttaggcctGTTGGTGTCGGTAAAGAAAA	ChrIV$_{567108-567655}$ for pBJL2889 and pBJL2890
OJL1797	gctcaaatgggagctcTACAAAATTGGGGATCATGG	ChrIV$_{567108-567655}$ for pBJL2889 and pBJL2890
OJL1798	gctcaaatgggcggccgcAAATGCCTTGAGAGTTAGCC	ChrIV$_{567656-568133}$ for pBJL2889 and pBJL2890
OJL1799	gctcaaatggaagctttctagaAGGTGTAGGCTCAAAACATA	ChrIV$_{567656-568133}$ for pBJL2889 and pBJL2890
OJL1804	gctcaaatggaagcttaggcctGAATAAACAGACACTTCCTG	ChrIV$_{1088500-1089039}$ for pBJL2891 and pBJL2892
OJL1805	gctcaaatgggagctcATGGAGGAACCTAAGCCTTC	ChrIV$_{1088500-1089039}$ for pBJL2891 and pBJL2892
OJL1806	gctcaaatgggcggccgcGAGGAGGATCACTTCTGCCC	ChrIV$_{1089040-1089633}$ for pBJL2891 and pBJL2892
OJL1807	gctcaaatggaagctttctagaATAGGTGAGGGAACACCTCA	ChrIV$_{1089040-1089633}$ for pBJL2891 and pBJL2892
OJL1852	AAAGGCATGCTGATTGTTGG	Hybrid Ty Junction Sequencing
OJL1853	GTTCAACAGAGAAGCCACAG	Hybrid Ty Junction Sequencing
OJL1955	TCATGCTTTTGAGTAACGGGTAATGACATACATTAGTGAC	Primer 1 for junction PCR
OJL1956	CTCTTCTTTACAGAAATACAAAAGGCATGCTGATTGTTGG	Primer 2 for junction PCR, Hybrid Ty Junction Sequencing
OJL1957	ACTGATGGTTCAACAGAGAAGCCACAGTTAAAAAAGGTCC	Primer 3 for junction PCR (amplicons 515-650kb), Hybrid Ty Junction Sequencing
OJL1958	TAGGAAAACGTACTGTGATTTTGAATACACTGGAATAGGG	Primer 4 for junction PCR (amplicons 515-650kb)
OJL1983	TTCACGATCCAAGCACTATTTGCCATTTTTGTGCCCTTTC	Primer 3 for junction PCR (amplicons 515-985kb)
OJL1984	GCGAGGCAGGCACCTAGTCTCTAAACCCTTCATATTGATC	Primer 4 for junction PCR (amplicons 515-985kb)
OJL2059	CAAACAAAGCTATGGCCTC	Hybrid Ty Junction Sequencing
OJL2081	GTATAAATTATTACCTGATAC	Hybrid Ty Junction Sequencing
OJL2082	CAAGAATAGGTGGATAATACGGTAATCGTATG	Hybrid Ty Junction Sequencing
OJL2083	CTCGAGTAATACCGCAGTGTCTTGACAATC	Hybrid Ty Junction Sequencing
OJL2087	GACTGAGGTTATTCAATAGCGGAATAGCTTC	Hybrid Ty Junction Sequencing
OJL2091	CAATGTTAGCGACAGATTGGCCTGTC	Hybrid Ty Junction Sequencing
OJL2092	GATCGGATGGTACAGTACTAGCTC	Hybrid Ty Junction Sequencing
OJL2093	GATTCTAGAGCACACGGTGTCGCTGAAC	Hybrid Ty Junction Sequencing
OJL2094	GAAGTTGATGCCGACATATCTGAATAC	Hybrid Ty Junction Sequencing
OJL2095	GAGAAGTCTGGAACCACCAAGATCGAAG	Hybrid Ty Junction Sequencing
OJL2096	CGACATGCAAGAAGTTCGCGGATGGTC	Hybrid Ty Junction Sequencing
OJL2097	gaactgaaggaaatagtaacggattatttaggtGAGCAGATTGTACTGAGAGTG	*dnl4::TRP1*, Step 1
OJL2098	caaaaaattaagcctccgcaaaacgcaccaGCATCTGTGCGGTATTTCAC	*dnl4::TRP1*, Step 1
OJL2099	gtggaaaataaatactaaaataaaaatctaGAACTGAAGGAAATAGTAACGG	*dnl4::TRP1*, Step 2
OJL2100	tacatatgtaggatagtattaaataaacttCAAAAAATTAAGCCTCCGC	*dnl4::TRP1*, Step 2
OJL2117	gaaggttctggtggctttggtgtgttgttgGAGCAGATTGTACTGAGAGTG	*rad52::TRP1*, Step 1
OJL2118	aatgatgcaaatttttatttgtttcggccaggaagcgttGCATCTGTGCGGTATTTCAC	*rad52::TRP1*, Step 1
OJL2119	atgcaaacaaggaggttgccaagaactgctGAAGGTTCTGGTGGCTTTGG	*rad52::TRP1*, Step 2
OJL2120	aactagaggattttggagtaataaatAATGATGCAAATTTTTTATTTGTTTCGGC	*rad52::TRP1*, Step 2
OJL2144	TCTGATGTTAAAGTGTGTGGTGG	Hybrid Ty Junction Sequencing
OJL2145	CATGAAGATTGGGTGAATTTTGAG	Hybrid Ty Junction Sequencing
OJL2146	GCAAGTGATTTTACGGAGGG	Hybrid Ty Junction Sequencing
OJL2147	CTGATAGTAGATCAACGATCAG	Hybrid Ty Junction Sequencing

Table S8

Plasmids used in this study.

Name	Description	Source
pAG25	*natMX*	Goldstein, A.L. et al. *Yeast* **15,** 1541-1553 (1999)
pBJL2889	*ChrIV*$_{567108\text{-}567655}$, *ade3-2p, kanMX, ChrIV*$_{567656\text{-}568133}$	This study
pBJL2890	*ChrIV*$_{567108\text{-}567655}$, *ade3-2p, ARS317, kanMX, ChrIV*$_{567656\text{-}568133}$	This study
pBJL2891	*ChrIV*$_{1088500\text{-}1089039}$, *ade3-2p, kanMX, ChrIV*$_{1089040\text{-}1089633}$	This study
pBJL2892	*ChrIV*$_{1088500\text{-}1089039}$, *ade3-2p, ARS317, kanMX, ChrIV*$_{1089040\text{-}108963}$	This study
pDK243	*ade3-2p, LEU2*	Koshland, D., et. al. *Cell* **40**, 393-403 (1985)
pFA6a-pGAL1-3HA	*kanMX*	Longtine, M.S. et al. *Yeast* **14,** 953-961 (1998)
pJL737	*ORC6, URA3*	Nguyen, V.Q. et al. *Nature* **411,** 1068-1073 (2001)
pJL806	*pGAL1, URA3*	Nguyen, V.Q. et al. *Nature* **411,** 1068-1073 (2001)
pJL1033	*MCM7, URA3*	Nguyen, V.Q. et al. *Curr Biol* **10,** 195-205 (2000)
pJL1206	*MCM7-2NLS, URA3*	Nguyen, V.Q. et al. *Nature* **411,** 1068-1073 (2001)
pJL1488	*pGAL1-ΔntCDC6-cdk2A, URA3*	Green, B.M. et al. *Mol Biol Cell* **17,** 2401-2414 (2005)
pMP933	*ORC2-(NotI-SgrAI), URA3*	Nguyen, V.Q. et al. *Nature* **411,** 1068-1073 (2001)
pRSS56	*Amp*^{R}	Sikorski, R.S. et al. *Genetics* **122,** 19-27 (1989)
pSB283	*pGAL-HO, LEU2, URA3, CEN7*	Berlin, V. et al. *Meth Enzymol* **194,** 774-792 (1991)

Table S9

Yeast strains used in this study.

Strain	Genotype	Source
4524-1-3	*MATα cdc7-1 leu2 ade2 ade3 his7 sap3 gal1 ura1 can1*	Palmer et al.[1]
4525-061	*MATα cdc6-1 leu2 ade2 ade3 his7 sap3 gal1 ura1 can1*	Palmer et al.[1]
4528-091	*MATα cdc9-1 leu2 ade2 ade3 his7 sap3 gal1 ura1 can1*	Palmer et al.[1]
4532-171	*MATα cdc17-1 leu2 ade2 ade3 his7 sap3 gal1 ura1 can1*	Palmer et al.[1]
4541-8-5	*MATα leu2 ade2 ade3 his7 sap3 gal1 ura1 can1*	Palmer et al.[1]
YJL1737	*MATa orc2-cdk6A orc6-cdk4A ura3-52 leu2 trp1-289 ade2 ade3 bar1::LEU2*	Nguyen et al.[2]
YJL2067	*MATa MCM7-2NLS orc2-cdk6A orc6-cdk4A ura3-52 leu2 trp1-289 ade2 ade3 bar1::LEU2*	This study
YJL3151	*MATa MCM7-2NLS ORC2 orc6-cdk4A ura3-52 leu2 trp1-289 ade2 ade3 bar1::LEU2*	This study
YJL3155	*MATa MCM7-2NLS ORC2 orc6-cdk1A$_{116}$ ura3-52 leu2 trp1-289 ade2 ade3 bar1::LEU2*	This study
YJL3165	*MATα MCM7-2NLS ORC2 orc6-cdk1A$_{116}$ ura3-52 leu2 trp1-289 ade2 ade3 bar1::LEU2*	This study
YJL3516	*MATa MCM7 ORC2 orc6-cdk1A$_{116}$ ura3-52 leu2 trp1-289 ade2 ade3 bar1::LEU2*	This study
YJL3519	*MATα MCM7 ORC2 orc6-cdk1A$_{116}$ ura3-52 leu2 trp1-289 ade2 ade3 bar1::LEU2*	This study
YJL3756	*MATa MCM7-2NLS ORC2 orc6-cdk1A$_{116}$ ura3-52::{pGAL, URA3} leu2 trp1-289 ade2 ade3 bar1::LEU2*	This study
YJL3758	*MATa MCM7-2NLS ORC2 orc6-cdk1A$_{116}$ ura3-52::{pGAL-ΔntCDC6-cdk2A, URA3} leu2 trp1-289 ade2 ade3 bar1::LEU2*	This study
YJL4486	*MATa MCM7-2NLS ORC2 orc6-cdk1A$_{116}$ ura3-52::{pGAL, URA3} leu2 trp1-289 ade2 ade3 bar1 ::LEU2 cdc20::{pMET3-HA3-CDC20, TRP1}*	Green et al.[3]
YJL6032	*MATa MCM7-2NLS ORC2 orc6-cdk1A$_{116}$ ura3-52::{pGAL-ΔntCDC6-cdk2A, URA3} leu2 trp1-289 ade2 ade3 bar1::LEU2 ChrIII$_{297kb}$::{ade3-2p, kanMX}*	This study
YJL6555	*MATa MCM7-2NLS ORC2 orc6-cdk1A$_{116}$ ura3-52::{pGAL-ΔntCDC6-cdk2A, URA3} leu2 trp1-289 ade2 ade3 bar1::LEU2 ChrIV$_{567kb}$::{ade3-2p, kanMX} ars317::natMX*	This study
YJL6557	*MATa MCM7-2NLS ORC2 orc6-cdk1A$_{116}$ ura3-52::{pGAL-ΔntCDC6-cdk2A, URA3} leu2 trp1-289 ade2 ade3 bar1::LEU2 ChrIV$_{1089kb}$::{ade3-2p, kanMX} ars317::natMX*	This study
YJL6558	*MATa MCM7-2NLS ORC2 orc6-cdk1A$_{116}$ ura3-52::{pGAL-ΔntCDC6-cdk2A, URA3} leu2 trp1-289 ade2 ade3 bar1::LEU2 ChrIV$_{567kb}$::{ade3-2p, ARS317, kanMX} ars317::natMX*	This study
YJL6561	*MATa MCM7-2NLS ORC2 orc6-cdk1A$_{116}$ ura3-52::{pGAL-ΔntCDC6-cdk2A, URA3} leu2 trp1-289 ade2 ade3 bar1::LEU2 ChrIV$_{1089kb}$::{ade3-2p, ARS317, kanMX} ars317::natMX*	This study
YJL6974	*MATa MCM7-2NLS ORC2 orc6-cdk1A$_{116}$ ura3-52::{pGAL, URA3} leu2 trp1-289 ade2 ade3 bar1::LEU2 ChrIV$_{567kb}$::{ade3-2p, ARS317, kanMX} ars317::natMX*	This study

Table S9 (continued)

Yeast strains used in this study.

Strain	Genotype	Source
YJL6977	*MATa MCM7-2NLS ORC2 orc6-cdk1A$_{116}$ ura3-52::{pGAL, URA3} leu2 trp1-289 ade2 ade3 bar1::LEU2 ChrIV$_{1089kb}$::{ade3-2p, ARS317, kanMX} ars317::natMX*	This study
YJL6993	*MATa MCM7 ORC2 orc6-cdk1A$_{116}$ ura3-52 leu2 trp1-289 ade2 ade3 bar1::LEU2 ChrIV$_{567kb}$::{ade3-2p, ARS317, kanMX}*	This study
YJL7002	*MATa/MATα leu2/leu2 ade2/ade2 ade3/ade3 his7/his7 sap3/sap3 gal1/gal1 ura1/ura1 can1/can1 ChrIV/ChrIV$_{567kb}$::{ade3-2p, ARS317, kanMX}*	This study
YJL7003	*MATa/MATα cdc6-1/cdc6-1 leu2/leu2 ade2/ade2 ade3/ade3 his7/his7 sap3/sap3 gal1/gal1 can1/can1 ChrIV/ChrIV$_{567kb}$::{ade3-2p, ARS317, kanMX}*	This study
YJL7005	*MATa/MATα cdc9-1/cdc9-1 leu2/leu2 ade2/ade2 ade3/ade3 his7/his7 sap3/sap3 gal1/gal1 ura1/ura1 can1/can1 ChrIV/ChrIV$_{567kb}$::{ade3-2p, ARS317, kanMX}*	This study
YJL7006	*MATa/MATα cdc17-1/cdc17-1 leu2/leu2 ade2/ade2 ade3/ade3 his7/his7 sap3/sap3 gal1/gal1 ura1/ura1 can1/can1 ChrIV/ChrIV$_{567kb}$::{ade3-2p, ARS317, kanMX}*	This study
YJL7007	*MATα/MATa leu2/leu2 ura3-52/ura3-52 trp1-289/trp1-289 ade2/ade2 ade3/ade3 bar1::LEU2/bar1::LEU2 ChrIV/ChrIV$_{567kb}$::{ade3-2p, ARS317, kanMX}*	This study
YJL7087	*MATa/MATα cdc7-1/cdc7-1 leu2/leu2 ade2/ade2 ade3/ade3 his7/his7 sap3/sap3 gal1/gal1 can1/can1 ChrIV/ChrIV$_{567kb}$::{ade3-2p, ARS317, kanMX}*	This study
YJL7443	*MATa dnl4::TRP1 MCM7-2NLS ORC2 orc6-cdk1A$_{116}$ ura3-52::{pGAL-ΔntCDC6-cdk2A, URA3} leu2 trp1-289 ade2 ade3 bar1::LEU2 ChrIV$_{567kb}$::{ade3-2p, ARS317, kanMX} ars317::natMX*	This study
YJL7452	*MATa rad52::TRP1 MCM7-2NLS ORC2 orc6-cdk1A$_{116}$ ura3-52::{pGAL-ΔntCDC6-cdk2A, URA3} leu2 trp1-289 ade2 ade3 bar1::LEU2 ChrIV$_{567kb}$::{ade3-2p, ARS317, kanMX} ars317::natMX*	This study
YJL7695	*MATa MCM7 ORC2 orc6-cdk1A$_{116}$ ura3-52 leu2 trp1-289 ade2 ade3 bar1::LEU2 ChrIV$_{567kb}$::{ade3-2p, ARS317, kanMX} ars317::natMX*	This study

[1] Palmer, R. E. et al. *Genetics* **125**, 763-774 (1990)

[2] Nguyen, V.Q. et al. *Nature* **411,** 1068-1073 (2001)

[3] Green, B.M. et al. *Mol Biol Cell* **17**, 2401-2414 (2006)

SUPPLEMENTARY REFERENCES

S1. I. F. Davidson, A. Li, J. J. Blow, Deregulated replication licensing causes DNA fragmentation consistent with head-to-tail fork collision. *Mol Cell* 24, 433 (2006).

S2. B. M. Green, R. J. Morreale, B. Ozaydin, J. L. Derisi, J. J. Li, Genome-wide mapping of DNA synthesis in Saccharomyces cerevisiae reveals that mechanisms preventing reinitiation of DNA replication are not redundant. *Mol Biol Cell* 17, 2401 (2006).

S3. V. Archambault, A. E. Ikui, B. J. Drapkin, F. R. Cross, Disruption of mechanisms that prevent rereplication triggers a DNA damage response. *Mol Cell Biol* 25, 6707 (2005).

S4. B. M. Green, J. J. Li, Loss of rereplication control in Saccharomyces cerevisiae results in extensive DNA damage. *Mol Biol Cell* 16, 421 (2005).

S5. M. Melixetian *et al.*, Loss of Geminin induces rereplication in the presence of functional p53. *J Cell Biol* 165, 473 (2004).

S6. C. Vaziri *et al.*, A p53-dependent checkpoint pathway prevents rereplication. *Mol Cell* 11, 997 (2003).

S7. K. Labib, B. Hodgson, Replication fork barriers: pausing for a break or stalling for time? *EMBO Rep* 8, 346 (2007).

S8. A. Aguilera, B. Gomez-Gonzalez, Genome instability: a mechanistic view of its causes and consequences. *Nat Rev Genet* 9, 204 (2008).

S9. R. D. Kolodner, C. D. Putnam, K. Myung, Maintenance of genome stability in Saccharomyces cerevisiae. *Science* 297, 552 (2002).

S10. T. Weinert, S. Kaochar, H. Jones, A. Paek, A. J. Clark, The replication fork's five degrees of freedom, their failure and genome rearrangements. *Curr Opin Cell Biol* 21, 778 (2009).

S11. F. J. Lemoine, N. P. Degtyareva, K. Lobachev, T. D. Petes, Chromosomal translocations in yeast induced by low levels of DNA polymerase a model for chromosome fragile sites. *Cell* 120, 587 (2005).

S12. V. Narayanan, P. A. Mieczkowski, H. M. Kim, T. D. Petes, K. S. Lobachev, The pattern of gene amplification is determined by the chromosomal location of hairpin-capped breaks. *Cell* 125, 1283 (2006).

S13. K. Umezu, M. Hiraoka, M. Mori, H. Maki, Structural analysis of aberrant chromosomes that occur spontaneously in diploid Saccharomyces cerevisiae: retrotransposon Ty1 plays a crucial role in chromosomal rearrangements. *Genetics* 160, 97 (2002).

S14. J. J. Blow, X. Q. Ge, A model for DNA replication showing how dormant origins safeguard against replication fork failure. *EMBO Rep* 10, 406 (2009).

S15. M. Botchan, W. Topp, J. Sambrook, Studies on simian virus 40 excision from cellular chromosomes. *Cold Spring Harb Symp Quant Biol* 43 Pt 2, 709 (1979).

S16. A. C. Spradling, The organization and amplification of two chromosomal domains containing Drosophila chorion genes. *Cell* 27, 193 (1981).

S17. D. G. Albertson, Gene amplification in cancer. *Trends Genet* 22, 447 (2006).

S18. P. J. Hahn, Molecular biology of double-minute chromosomes. *Bioessays* 15, 477 (1993).

S19. E. Wintersberger, DNA amplification: new insights into its mechanism. *Chromosoma* 103, 73 (1994).

S20. M. Debatisse, B. Malfoy, Gene amplification mechanisms. *Adv Exp Med Biol* 570, 343 (2005).

S21. J. Herrick *et al.*, Genomic organization of amplified MYC genes suggests distinct mechanisms of amplification in tumorigenesis. *Cancer Res* 65, 1174 (2005).

S22. Y. Kuwahara *et al.*, Alternative mechanisms of gene amplification in human cancers. *Genes Chromosomes Cancer* 41, 125 (2004).

S23. J. O'Neil *et al.*, Alu elements mediate MYB gene tandem duplication in human T-ALL. *J Exp Med* 204, 3059 (2007).

S24. M. P. Strout, G. Marcucci, C. D. Bloomfield, M. A. Caligiuri, The partial tandem duplication of ALL1 (MLL) is consistently generated by Alu-mediated homologous recombination in acute myeloid leukemia. *Proc Natl Acad Sci U S A* 95, 2390 (1998).

S25. P. J. Stephens *et al.*, Complex landscapes of somatic rearrangement in human breast cancer genomes. *Nature* 462, 1005 (2009).

S26. J. Kim, H. Feng, E. T. Kipreos, C. elegans CUL-4 prevents rereplication by promoting the nuclear export of CDC-6 via a CKI-1-dependent pathway. *Curr Biol* 17, 966 (2007).

S27. H. Nishitani, P. Nurse, p65cdc18 plays a major role controlling the initiation of DNA replication in fission yeast. *Cell* 83, 397 (1995).

S28. M. Thomer, N. R. May, B. D. Aggarwal, G. Kwok, B. R. Calvi, Drosophila double-parked is sufficient to induce re-replication during development and is regulated by cyclin E/CDK2. *Development* 131, 4807 (2004).

S29. L. A. Loeb, J. H. Bielas, R. A. Beckman, Cancers exhibit a mutator phenotype: clinical implications. *Cancer Res* 68, 3551 (2008).

S30. E. Arentson *et al.*, Oncogenic potential of the DNA replication licensing protein CDT1. *Oncogene* 21, 1150 (2002).

S31. M. Liontos *et al.*, Deregulated overexpression of hCdt1 and hCdc6 promotes malignant behavior. *Cancer Res* 67, 10899 (2007).

S32. J. Seo *et al.*, Cdt1 transgenic mice develop lymphoblastic lymphoma in the absence of p53. *Oncogene* 24, 8176 (2005).

S33. H. Innan, F. Kondrashov, The evolution of gene duplications: classifying and distinguishing between models. *Nat Rev Genet* 11, 97 (2010).

S34. F. Zhang, W. Gu, M. E. Hurles, J. R. Lupski, Copy number variation in human health, disease, and evolution. *Annu Rev Genomics Hum Genet* 10, 451 (2009).

S35. R. T. Schimke, S. W. Sherwood, A. B. Hill, R. N. Johnston, Overreplication and recombination of DNA in higher eukaryotes: potential consequences and biological implications. *Proc Natl Acad Sci U S A* 83, 2157 (1986).

S36. E. Loh, J. J. Salk, L. A. Loeb, Optimization of DNA polymerase mutation rates during bacterial evolution. *Proc Natl Acad Sci U S A* 107, 1154 (2010).

S37. M. S. Longtine *et al.*, Additional modules for versatile and economical PCR-based gene deletion and modification in Saccharomyces cerevisiae. *Yeast* 14, 953 (1998).

S38. D. Koshland, J. C. Kent, L. H. Hartwell, Genetic analysis of the mitotic transmission of minichromosomes. *Cell* 40, 393 (1985).

S39. R. S. Sikorski, P. Hieter, A system of shuttle vectors and yeast host strains designed for efficient manipulation of DNA in Saccharomyces cerevisiae. *Genetics* 122, 19 (1989).

S40. V. Q. Nguyen, C. Co, J. J. Li, Cyclin-dependent kinases prevent DNA re-replication through multiple mechanisms. *Nature* 411, 1068 (2001).

S41. A. L. Goldstein, J. H. McCusker, Three new dominant drug resistance cassettes for gene disruption in Saccharomyces cerevisiae. *Yeast* 15, 1541 (1999).

S42. V. Q. Nguyen, C. Co, K. Irie, J. J. Li, Clb/Cdc28 kinases promote nuclear export of the replication initiator proteins Mcm2-7. *Curr Biol* 10, 195 (2000).

S43. V. Berlin, J. A. Brill, J. Trueheart, J. D. Boeke, G. R. Fink, Genetic screens and selections for cell and nuclear fusion mutants. *Methods Enzymol* 194, 774 (1991).

S44. R. E. Palmer, E. Hogan, D. Koshland, Mitotic transmission of artificial chromosomes in cdc mutants of the yeast, Saccharomyces cerevisiae. *Genetics* 125, 763 (1990).

S45. F. Sherman, Getting started with yeast. *Methods Enzymol* 350, 3 (2002).

S46. S. B. Haase, S. I. Reed, Improved flow cytometric analysis of the budding yeast cell cycle. *Cell Cycle* 1, 132 (2002).

S47. D. E. Lea, C. A. Coulson, The distribution of the number of mutants in bacterial populations. *J. Genetics* 49, 264 (1949).

S48. J. A. Pleiss, G. B. Whitworth, M. Bergkessel, C. Guthrie, Transcript specificity in yeast pre-mRNA splicing revealed by mutations in core spliceosomal components. *PLoS Biol* 5, e90 (2007).

S49. C. S. Hoffman, F. Winston, A ten-minute DNA preparation from yeast efficiently releases autonomous plasmids for transformation of Escherichia coli. *Gene* 57, 267 (1987).

S50. J. M. Cherry *et al.*, Genetic and physical maps of Saccharomyces cerevisiae. *Nature* 387, 67 (1997).